The Astrophysical Journal, 653:621–635, 2006 December 10

AN OBSERVATIONAL STUDY OF TIDAL SYNCHRONIZATION IN SOLAR-TYPE BINARY STARS IN THE OPEN CLUSTERS M35 AND M34[1]

Søren Meibom[2,3] and Robert D. Mathieu[3]
Astronomy Department, University of Wisconsin–Madison, Madison, WI 53706

and

Keivan G. Stassun[3]
Physics and Astronomy Department, Vanderbilt University, Nashville, TN 32735
Received 2006 February 21; accepted 2006 August 6

ABSTRACT

We present rotation periods for the solar-type primary stars in 13 close ($a \lesssim 5$ AU) single-lined spectroscopic binaries with known orbital periods (P) and eccentricities (e). All binaries are members of the open clusters M35 (NGC 2168; ~150 Myr) and M34 (NGC 1039; ~250 Myr). The binary orbital parameters and the rotation periods of the primary stars were determined from time-series spectroscopy and time-series photometry, respectively. Knowledge of the ages, orbital periods, and eccentricities of these binaries combined with the rotation periods and masses of their primary stars makes them particularly interesting systems for studying the rates of tidal circularization and synchronization. Our sample of 13 binaries includes six with orbital periods shortward of 13 days ($a \lesssim 0.12$ AU). The stars in these binaries orbit sufficiently close that their spins and orbits have evolved toward synchronization and circularization due to tidal interactions. We investigate the degree of tidal synchronization in each binary by comparing the angular rotation velocity of the primary stars ($\Omega_\star$) to the angular velocity expected if the primary star was synchronized ($e = 0$) or pseudosynchronized ($e > 0$) with the orbital motion ($\Omega_{\rm ps}$). Of the six closest binaries, two with circular orbits are not synchronized, one being subsynchronous and one being supersynchronous, and the primary stars in two binaries with eccentric orbits are rotating more slowly than pseudosynchronism. The remaining two binaries have reached the equilibrium state of both a circularized orbit and synchronized rotation. As a set, the six binaries present a challenging case study for tidal evolution theory, which in particular does not predict subsynchronous rotation in such close systems.

Subject headings: binaries: spectroscopic — open clusters and associations: general — stars: rotation

1. INTRODUCTION

Tidal and dissipative forces in close detached binary stars drive an exchange of angular momentum between the rotation of the stars and their orbital motion. The cumulative effects of such tidal interactions with time is referred to as tidal evolution. The characteristic signs of tidal evolution are (1) alignment of the stellar spin axes perpendicular to the orbital plane; (2) synchronization of the rotation of the stars to the orbital motion; and (3) circularization of the orbits. In a population of coeval detached late-type binary stars, tidal evolution can be observed among the closest binaries ($a \lesssim 0.2$ AU).

Observations of "tidal circularization" have been the primary constraint on tidal theory over the past two decades (e.g., Meibom & Mathieu 2005; Mathieu et al. 1992, 2004; Latham et al. 2002; Melo et al. 2001; Duquennoy et al. 1992). In particular, the distribution of orbital eccentricities with orbital periods [the e-log (P) diagram] has provided clear evidence for tidal circularization in homogeneous and coeval populations of late-type binaries and enabled a robust measure of the degree of circularization integrated over the lifetime of the binary population as a function of orbital period. Meibom & Mathieu (2005) define the "tidal circularization period" of a binary population as the longest orbital period to which binaries with initial eccentricities of $e = 0.35$ circularize at the age of the population. Importantly, current theories of tidal circularization cannot account for the distribution of tidal circularization periods with population age.

In comparison, the amount of observational data suitable for measuring the rate of "tidal synchronization" in late-type binaries is sparse. This is in part because binary orbital elements are simpler to obtain than rotation periods for stars in binaries. Even so, observations of the synchronization of the stars in a binary system provide a second window on the tidal effects on that system, and one of major importance for several reasons. First, tidal theory makes explicit predictions for the relative rates of tidal circularization and synchronization that can be straightforwardly tested (Witte & Savonije 2002; Zahn & Bouchet 1989). For a typical binary the two rates differ and the predicted evolutionary paths from an asynchronous, eccentric binary to a synchronized and circular binary take the stars in and out of synchronism during the evolutions of the stars, their orbital separation, and their orbital eccentricity (see Fig. 1 in Zahn & Bouchet [1989] and Figs. 1 and 3 in Witte & Savonije [2002]). Second, the range in binary separations over which tidal synchronization can significantly affect the stellar angular momentum evolution provides an important constraint on the impact of binarity on stellar angular momentum evolution in late-type stars. Third, synchronization of the observable surface layers is closely linked to the internal angular momentum transport in the star. Thus, the rate of synchronization of the surface layers can shed light on the coupling between those layers and the stellar interior. Fourth, observations of magnetic

[1] WIYN Open Cluster Study. XXIX.

[2] Current affiliation: Harvard-Smithsonian Center for Astrophysics, 60 Garden Street, Cambridge, MA 02138; smeibom@cfa.harvard.edu.

[3] Visiting Astronomer, Kitt Peak National Observatory, National Optical Astronomy Observatory, which is operated by the Association of Universities for Research in Astronomy, Inc. (AURA) under cooperative agreement with the National Science Foundation.

field tracers (e.g., X-rays, chromospheric emission) during rapid stellar evolution in tidally synchronized binaries may enable determination of the evolution rates of stellar dynamos.

Finally, significant tidal synchronization and circularization is expected in the many star-planet systems where the planets orbit very close to their late-type host stars (i.e., "hot Jupiter" systems). Tidal interactions in star-planet systems may therefore play an important role in determining the observed distributions of mass, orbital period, and eccentricity of extrasolar planets (e.g., Ogilvie & Lin 2004).

To date, most published studies of synchronization have focused on early-type binaries (e.g., Abt & Boonyarak 2004; Abt et al. 2002; Giuricin et al. 1984a, 1984b; Levato 1974). This emphasis is due, in part, to telescope and instrument capabilities, which in the past have favored bright and rapidly rotating stars. In addition, the use of archived data on eclipsing binaries has introduced a bias toward higher mass stars.

However, a few recent studies of tidal synchronization, e.g., Giuricin et al. (1984c), Claret et al. (1995), and Claret & Cunha (1997), include binaries with late-type main-sequence primary stars. These studies represent important contributions to the study of tidal synchronization. Giuricin et al. studied 43 detached double-lined eclipsing and noneclipsing binaries with at least one late-type stellar component. They found that the observed degree of synchronism was in agreement with the theoretical predictions of Zahn (1977). In half of the binaries in their study the primary or secondary star, or both, have evolved off the main sequence and stellar rotation was derived from either line-broadening [$v \sin(i)$] or periodic brightness variations. For the noneclipsing binaries in their study, the stellar rotation velocities measured from line broadening are less suitable for constraining models of tidal synchronization, because of the ambiguities introduced by the unknown inclination of the rotation axis and nonrotational line broadening due to the secondary spectrum.

Claret et al. (1995) and Claret & Cunha (1997) studied tidal synchronization using eclipsing binary data from Andersen (1991), of which 10 systems have late-type stellar components. The two studies compared the observed binary parameters against the model predictions of Tassoul (1987, 1988) and Zahn (1989), respectively, and found general agreement between the observed level of synchronization and the predicted timescales for synchronization. Astrophysical parameters required to determine the theoretical timescale for which synchronization is achieved were obtained by comparing theoretical models (Claret 1995; Claret & Gimenez 1995) directly to each star of the Andersen sample. Rotation velocities [$v \sin(i)$] for all stars were derived from line broadening.

Knowledge of binary ages is critical in order to measure the rate and evolution of tidal synchronization. Furthermore, because of the sensitive dependence of tidal effects to stellar radius, knowledge of the stellar evolutionary state and history is essential for testing tidal evolution. For example, tidal theory predicts that the pre–main sequence (PMS) and the early main sequence ($t \lesssim 500$ Myr) are the most active phases of tidal evolution. The PMS phase because of the large radii and deep convective envelopes, and the early main-sequence phase because the stars are spinning supersynchronously after contracting onto the zero-age main sequence. Similarly, post–main-sequence evolution of one or both components of a binary greatly increases the rate of tidal evolution.

Thus, an optimal binary sample for the study of tidal evolution would comprise a coeval population of late-type binaries with accurate information about age, evolutionary stage, orbital parameters, and rotational angular velocities of the stars. Arguably such binary samples with ages $t \lesssim 500$ Myr are particularly interesting. Given these needs, young open clusters are superb laboratories for the study of tidal evolution.

So motivated, we have undertaken parallel spectroscopic and photometric surveys of the open clusters M35 ($\alpha_{2000} = 6^{\rm h}9^{\rm m}$, $\delta_{2000} = 24^\circ 20'$) and M34 ($\alpha_{2000} = 2^{\rm h}42^{\rm m}$, $\delta_{2000} = 42^\circ 46'$) to derive orbital periods and eccentricities as well as stellar rotation periods for late-type binary stars. The goal of this study is to measure the degree of tidal synchronization of the primary stars in the closest binaries ($a \lesssim 0.2$ AU) and to compare the results to the predictions from tidal theory.

M35 (150 Myr; von Hippel et al. 2002; C. P. Deliyannis 2006, in preparation) and M34 (250 Myr; A. Steinhauer 2006, in preparation) provide populations of close late-type binaries with ages during the most active phase of tidal evolution, making them attractive targets for observational testing of models of tidal synchronization. M35, in particular, provides a rich population of close binaries that has allowed determination of a well-defined tidal circularization period at $10.2^{+1.0}_{-1.5}$ days (Meibom & Mathieu 2005). Indeed, eight out of the nine M35 binaries with periods less than $\sim$10 days have been circularized to eccentricities less than 0.05. In M34, our ongoing spectroscopic survey has led to the discovery of five circular binaries ($e < 0.1$) with periods of less than 5.5 days. A tidal circularization period has not yet been determined for M34.

We begin by briefly introducing the current theories of tidal evolution in § 2. Section 3 outlines our observational program, and § 4 describe our observational results. In § 5 we address potential complications of measuring the rotation periods of stars in close binary systems. In § 6 we evaluate the degree of tidal synchronization and circularization for the closest binaries in M35 and M34 and introduce the log ($\Omega_\star/\Omega_{\rm ps}$)-log ($P$) diagram, which presents the dependence on stellar separation. We compare the observed tidal evolution of individual binaries to the predictions of current tidal theory in § 7. Section 8 summarizes and presents our conclusions.

2. MODEL PREDICTIONS OF TIDAL SYNCHRONIZATION

Later in the paper we will discuss our observational results in the context of theoretical models of tidal evolution in solar-type binaries. The equilibrium tide theory (Zahn 1977, 1989; Hut 1981) has been the primary theory used to explain tidal evolution in main-sequence binaries with late-type components and was extended by Zahn & Bouchet (1989) to include tidal evolution during PMS evolution. The physical mechanism responsible for tidal dissipation is turbulent viscosity in the outer convective layers of binary component stars. Alternatively, the dynamical tide theory (Zahn 1975, 1977), which before 1998 was used primarily to explain tidal evolution in binaries with early-type stars, has recently been applied to binaries with solar-type components (Witte & Savonije 2002; Savonije & Witte 2002; Terquem et al. 1998; Goodman & Dickson 1998). In the dynamical tide theory, tidally induced internal gravity modes are thermally damped and dissipated in the convective envelope.

In the equilibrium tide theory, the characteristic times for tidal synchronization and circularization are (Zahn 1989)

$$t_{\rm sync} = \frac{t_{\rm diss}}{6\lambda_{\rm sync} q^2} \frac{I}{MR^2} \left(\frac{a}{R}\right)^6, \quad (1)$$

$$t_{\rm circ} = \frac{t_{\rm diss}}{21\lambda_{\rm circ} q(1+q)} \left(\frac{a}{R}\right)^8. \quad (2)$$

Both times are strongly dependent on the ratio of the stellar separation (a) to the stellar radius (R) and thus restrict significant tidal evolution to the closest binaries. M and I denote the mass and moment of inertia of the primary star, q the binary mass ratio, $t_{\rm diss}$ the viscous dissipation time, and $\lambda_{\rm sync/circ}$ a structural constant whose value depends on the mass concentration within the stars and on where in the star the tidal torque is applied.

From the ratio of equations (1) and (2) it can be estimated that $t_{\rm circ} \simeq 10^2$–$10^3 t_{\rm sync}$ for a binary with solar-type components. The process of tidal synchronization thus proceeds much faster than tidal circularization. This difference in timescales is primarily because the angular momenta of the individual stars ($\sim I\Omega \ll MR^2\Omega$) are much smaller than that of the orbit ($\sim Ma^2\omega$). Here ω and Ω are the orbital angular velocity and the stellar rotation angular velocity, respectively. A similar difference in the timescales for tidal circularization and synchronization is found in the dynamical tide theory (see, e.g., eqs. [41] and [42] in Terquem et al. 1998). On the basis of the finding from theory of a much shorter timescale for tidal synchronization than for circularization, it is expected that, at times when stellar structure is roughly constant over tidal evolution timescales (such as after the zero-age main sequence [ZAMS]), eccentric binaries will come to synchronization faster than circularization.

During this process, the stars in an eccentric binary will first synchronize their spin angular velocities to a value $\Omega_{\rm ps}$, close to (within $\sim$20%) the orbital angular velocity at periastron passage (ω_p), where the stellar separation is minimum. This is referred to as pseudosynchronization. An expression for $\Omega_{\rm ps}$ can be derived by setting the tidal torque on the stars integrated over the eccentric orbit equal to zero. In the weak friction (constant time lag) approximation (see Hut 1981),

$$\Omega_{\rm ps} = \frac{1 + (15/2)e^2 + (45/8)e^4 + (5/16)e^6}{(1+e)^2[1 + 3e^2 + (3/8)e^4]}\omega_p, \qquad (3)$$

$$\omega_p = \omega \frac{(1+e)^2}{(1-e^2)^{3/2}}. \qquad (4)$$

Thus, again when stellar structure is roughly constant, it is expected from tidal theory that the rotation of a star in an eccentric binary should be pseudosynchronized ($\Omega_\star = \Omega_{\rm ps}$) if the orbital period is similar to or shorter than the tidal circularization period.

More specific predictions for the evolution of tidal synchronization and circularization have been made in Zahn & Bouchet (1989; equilibrium tide theory) and Witte & Savonije (2002; dynamical tide theory) assuming specified sets of initial stellar and binary conditions. A detailed graphical illustration of the tidal evolution of a binary with two 1.0 $M_\odot$ stars is given by Zahn & Bouchet (1989). In their model, synchronization and circularization are achieved in less than 100,000 years due to large radii and deep convection during the PMS phase. The stars then spin up due to less efficient tidal braking as the convection retreats and the stars contract onto the ZAMS. Thus, at ages comparable to those of M35 and M34, Zahn & Bouchet predict supersynchronous rotation in circularized binaries at the ZAMS. Once the stars have settled on the main sequence, synchronization resumes and is completed by an age of $\sim$1 Gyr. Witte & Savonije present in their Figures 1 and 3 the tidal evolution of a binary with two 1.0 $M_\odot$ stars in the framework of the dynamical tide theory. In their model, starting at the ZAMS, pseudosynchronization is gradually achieved within $\sim$500 Myr.

The observational data presented in this paper provide orbital periods and eccentricities as well as stellar rotation periods for 13 main-sequence binaries with known ages. We are thus equipped to compare our observations of tidal evolution to the predictions derived from the findings of tidal theory.

3. OBSERVATIONS AND DATA REDUCTION

We have conducted two parallel observational programs on the open clusters M35 and M34: (1) high-precision radial velocity surveys to identify binaries and determine their orbital parameters; (2) comprehensive photometric time-series surveys to determine stellar rotation periods from light modulation by star spots on the surfaces of the late-type primary stars.

3.1. *Time-Series Spectroscopy*

M35 and M34 have been included in the WIYN Open Cluster Study (WOCS; Mathieu 2000) since 1997 and 2001, respectively. As part of WOCS, the solar-type stars in both clusters have been targets in extensive radial velocity surveys to determine cluster membership and to detect binary stars. A detailed description of the radial velocity surveys of these two clusters will follow in later papers; we give here the most relevant information.

All spectroscopic data were obtained using the WIYN[4] 3.5 m telescope at Kitt Peak, Arizona. The telescope is equipped with a Multi-Object Spectrograph (MOS) consisting of a fiber optic positioner (Hydra) feeding a bench-mounted spectrograph. The Hydra positioner is capable of placing $\sim$95 fibers in a 1° diameter field with a precision of 0.″2. In the field of M35 and M34 approximately 82–85 fibers are positioned on stars while the remaining fibers are used for measurements of the sky background. We use the 3″ diameter fibers optimized for blue transmission, and the spectrograph is configured with an echelle grating and an all-transmission optics camera providing high throughput at a resolution of $\sim$20,000. All observations were done at central wavelengths of 5130 or 6385 Å with a wavelength range of $\sim$200 Å providing rich arrays of narrow absorption lines. Radial velocities with a precision of $\lesssim$0.5 km s^{-1} are derived from the spectra via cross-correlation with a high-S/N sky spectrum (Hole et al. 2006; Meibom et al. 2001).

The initial selection of target stars was based on photometric cluster membership in the color-magnitude diagrams (CMDs; see Fig. 1). For M35 proper-motion membership studies to $V \lesssim 15$ by McNamara & Sekiguchi (1986) and Cudworth (1971) were used as well. The target list for M35 includes stars of type mid-F to mid-K, corresponding to a range in stellar mass from $\sim$1.4 $M_\odot$ [$V_0 \simeq 12.5, (B-V)_0 \simeq 0.4$] to $\sim$0.7 $M_\odot$ [$V_0 \simeq 16, (B-V)_0 \simeq 1.1$], with solar-mass stars at $V_0 \sim 15$. In M34 stars of type early-F to early-M were observed corresponding to a range in stellar mass from $\sim$1.5 $M_\odot$ [$V_0 \simeq 12.0$, $(B-V)_0 \sim 0.3$] to $\sim$0.4 $M_\odot$ [$V_0 \simeq 16.5$, $(B-V)_0 \sim 1.5$], with solar-mass stars at $V_0 \sim 13.5$.

Telescope time granted from Wisconsin and NOAO[5] allowed for three to four spectroscopic observing runs per year per cluster, with each run typically including multiple observations on several sequential nights. Once identified, velocity variables are observed at a frequency appropriate to the timescale of their variation. At present the radial velocity survey of M35 has resulted in a sample of 50 spectroscopic binaries for which orbital solutions have been derived. The orbital periods span 2.25–3112 days, corresponding to separations from 0.04 to $\sim$5 AU, assuming a

[4] The WIYN Observatory is a joint facility of the University of Wisconsin—Madison, Indiana University, Yale University, and the National Optical Astronomy Observatory.

[5] NOAO is the national center for ground-based nighttime astronomy in the United States and is operated by the Association of Universities for Research in Astronomy (AURA), Inc. under cooperative agreement with the National Science Foundation.

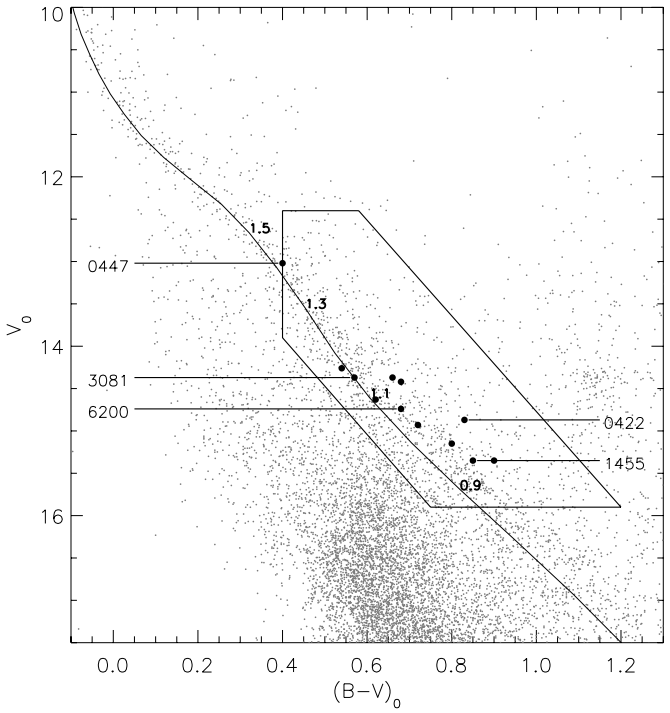

FIG. 1.—Color-magnitude diagram of M35. The photometry and the cluster reddening ($E_{(B-V)} = 0.2$) were provided by C. P. Deliyannis (2006, in preparation). The 12 binaries with known rotation periods of their primary stars are marked as black dots. The five binaries with orbital period shortward of 13 days are labeled with the last four digits of their respective 2MASS IDs. The 150 Myr isochrone overplotted has been corrected for reddening and extinction and a distance modulus of 9.8 (Kalirai et al. 2003). Relevant isochrone masses are marked. The stars included in our spectroscopic survey fall within the region outlined.

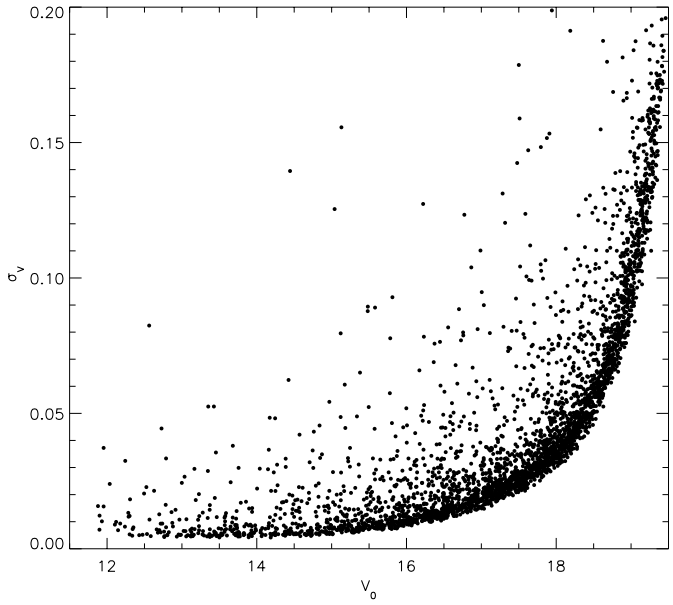

FIG. 2.—Standard deviation of the instrumental V magnitudes as a function of the true V magnitude (V_0) for stars in the field of M35. A first-order estimate of the true V magnitude has been obtained by applying a correction of -3.238 mag, equivalent to the mean difference between the instrumental V magnitude and the V magnitude from C. P. Deliyannis (2006, in preparation) plus an extinction correction of $3E_{(B-V)} = 0.6$ mag (C. P. Deliyannis 2006, in preparation). A relative photometric precision of $\sim$0.5% is obtained for stars with $12.0 \lesssim V \lesssim 15.0$.

1 $M_\odot$ primary star and a 0.5 $M_\odot$ secondary star. In M34 orbital parameters have been derived for 20 spectroscopic binaries spanning orbital periods from 2.26 to 1210 days. This paper is based on a subset of those binaries that are described in detail below.

3.2. *Time-Series Photometry*

We have photometrically surveyed stars in a $\sim 40' \times 40'$ region centered on M35 and M34. The photometric data were obtained using the WIYN 0.9 m telescope[6] at Kitt Peak equipped with a $2k \times 2k$ CCD camera. The complete data set is composed of images from two different but complementary observing programs. Images of the two clusters were acquired by the first author from 2002 December 1 to 17 with a frequency of approximately once per hour for $\sim$six hours per night that the clusters airmasses were below 1.5. In addition, one image per night was obtained in a queue-scheduled observing program from 2002 October to 2003 March. We reduced our CCD frames using the standard IRAF CCDRED package. We used the IRAF GASP package to compute a simple linear transformation of pixel coordinates to equatorial coordinates for each frame, using as reference approximately 30 stars from the Digitized Sky Survey per frame. Our derived stellar positions show a frame-to-frame scatter of less than 0.″1 in each direction. We identified stellar sources using the IRAF DAOFIND task and performed PSF photometry using the DAOPHOT package. The procedures used were described and developed in Stassun et al. (1999, 2002). Figure 2 displays the standard deviation as a function of V magnitude for stars in the field of M35. A relative photometric precision of $\sim$0.5% is obtained for stars with $12 \lesssim V \lesssim 15$, with slightly poorer precision at the $V = 16.5$ mag faint limit of the spectroscopic study. For M35 the result of the photometric survey is a database of differential photometric V-band light curves for $\sim$14,000 stars with $12 \lesssim V_0 \lesssim 19.5$. At the present time only the photometric data on M35 have been reduced and analyzed. The photometry for star 6211 in M34 presented in this paper is kindly provided by S. A. Barnes (2005), private communication.

We employed the Scargle (1982) periodogram analysis to detect periodic variability in the light curves (see Stassun et al. 1999). For each candidate star, we generate a set of 100 synthetic light curves, each consisting of normally distributed noise with a nightly and a night-to-night dispersion representative of our data. A periodogram was computed for each test light curve and the maximum of the 100 observed power levels was adopted as the level of 1% false-alarm probability (FAP). This measured FAP was used as the criterion for accepting or rejecting detected photometric variability; we accept only periods whose maximum periodogram signals are stronger than the power corresponding to the 1% FAP level. From our database we have determined stellar rotation periods for 443 stars. Of these, 259 have one or more radial velocity measurements (the remainder being below the faint limit of the spectroscopic survey or photometric nonmembers), 203 are photometric and spectroscopic members of M35, and 12 are members of binary systems with known orbital parameters. S. Meibom et al. (2006, in preparation) present and describe in more detail our photometric data, the reduction thereof, and the methods used for detecting periodic variability.

4. OBSERVATIONAL RESULTS

We present the spectroscopic and photometric results for 12 binaries in M35 and one binary in M34. These binaries are single-lined spectroscopic systems with well-determined orbital periods

[6] The 0.9 m telescope is operated by WIYN Inc. on behalf of a Consortium of 10 partner Universities and Organizations (see http://www.noao.edu/0.9m/general.html).

TABLE 1

PHOTOMETRIC AND SPECTROSCOPIC OBSERVATIONAL RESULTS

ID[a]	V_0	$(B-V)_0$	γ (km s^{-1})	$P_{\rm orbit}$ (days)	e	σ_e	$P_{\rm rot}^{\rm prim}$ (days)	$\delta(P_{\rm rot}^{\rm prim})$[b] (days)	$M_{\rm prim}$ ($M_\odot$)	ω[c] (rad day^{-1})	$\Omega_\star$[d] (rad day^{-1})	$\Omega_\star/\Omega_{\rm ps}$[e]	$\log(\Omega_\star/\Omega_{\rm ps})$	$P_{\rm RV}$[f] (%)
06090257+2420447	13.016	0.403	−8.30	10.28	0.009	0.019	2.30	0.02	1.4	0.611	2.73	4.46	0.65	94
06090306+2420095	14.369	0.655	−6.92	3112.67	0.394	0.118	2.48	0.01	1.1	0.002	2.54	625.66	2.80	90
06090306+2419361	15.150	0.802	−9.25	637.03	0.234	0.025	4.70	0.07	1.0	0.010	1.34	101.74	2.01	91
06090352+2417234	15.351	0.896	−6.74	156.60	0.580	0.034	2.38	0.02	0.9	0.040	2.64	17.52	1.24	88
06091557+2410422	14.867	0.834	−6.14	8.17	0.649	0.022	3.71	0.06	0.9	0.769	1.69	0.44	−0.35	76
06091924+2417223	14.933	0.724	−8.86	795.30	0.255	0.056	5.25	0.08	1.0	0.008	1.20	108.47	2.04	93
06092436+2426200	14.741	0.678	−7.36	10.33	0.016	0.009	10.13	0.39	1.1	0.609	0.62	1.02	0.01	93
06095563+2417454	14.420	0.680	−7.54	30.13	0.273	0.005	2.84	0.03	1.1	0.209	2.22	7.29	0.86	94
06085441+2403081	14.368	0.565	−7.45	12.28	0.550	0.003	6.03	0.12	1.1	0.512	1.04	0.61	−0.21	93
06082017+2421514	14.259	0.544	−8.16	2324.11	0.199	0.093	2.56	0.02	1.2	0.003	2.45	731.43	2.86	94
06074436+2430262	14.634	0.624	−7.04	476.21	0.389	0.046	4.26	0.07	1.1	0.013	1.48	56.47	1.75	91
06083789+2431455	15.354	0.855	−8.08	2.25	0.010	0.008	2.29	0.02	0.9	2.794	2.74	0.98	−0.01	93
02410619+4246211[g]	15.323	1.000	−7.27	4.39	0.063	0.033	8.03	0.10	0.7	1.431	0.78	0.53	−0.28	94

[a] Stellar 2MASS ID.
[b] The estimated uncertainty of the stellar rotation period [$\delta(P_{\rm rot}^{\rm prim})$].
[c] Average orbital angular velocity.
[d] Measured rotational angular velocity of the primary star.
[e] Ratio of the measured rotational angular velocity to the expected pseudosynchronous rotational angular velocity.
[f] The radial velocity membership probability ($P_{\rm RV}$) calculated using the formalism by Vasilevskis et al. (1958); see text.
[g] M34 binary.

($\sigma_{P_{\rm orb}}/P_{\rm orb} \lesssim 0.01$) and eccentricities ($\sigma_e \lesssim 10^{-2}$). The rotation periods of their primary stars are determined from periodic variations in their light curves, presumably due to spots on the stellar surfaces. The mass of the primary star in each binary has been estimated from 150 and 250 Myr Yale isochrones (Yi et al. 2003) fitted to the cluster sequences of M35 and M34, respectively. Photometry and values for cluster reddening for both clusters were provided by C. P. Deliyannis (2006, in preparation) and A. Steinhauer (2006, in preparation). Table 1 lists all observational results for the 13 binaries together with the derived orbital angular velocities and stellar rotation angular velocities needed for studying tidal synchronization. Figure 1 shows the CMD of M35. The locations of these 12 binaries are marked as black dots. Five M35 binaries discussed in detail below are labeled with the last four digits of their respective 2MASS IDs (see Table 1). The 150 Myr isochrone is corrected for reddening and extinction and a distance modulus of 9.8 (Kalirai et al. 2003). Relevant model masses are marked along the isochrone.

All 13 binaries are photometric and radial velocity members of M35 or M34. Figure 3 shows the distributions of measured radial velocities for the two clusters. Gaussian functions have been simultaneously fitted to the cluster and field components of each distribution. The radial velocity cluster membership probability ($P_{\rm RV}$) of each of the 13 binary stars is calculated following the formalism by Vasilevskis et al. (1958):

$$P_{\rm RV} = \frac{C({\rm RV})}{C({\rm RV}) + F({\rm RV})}, \tag{5}$$

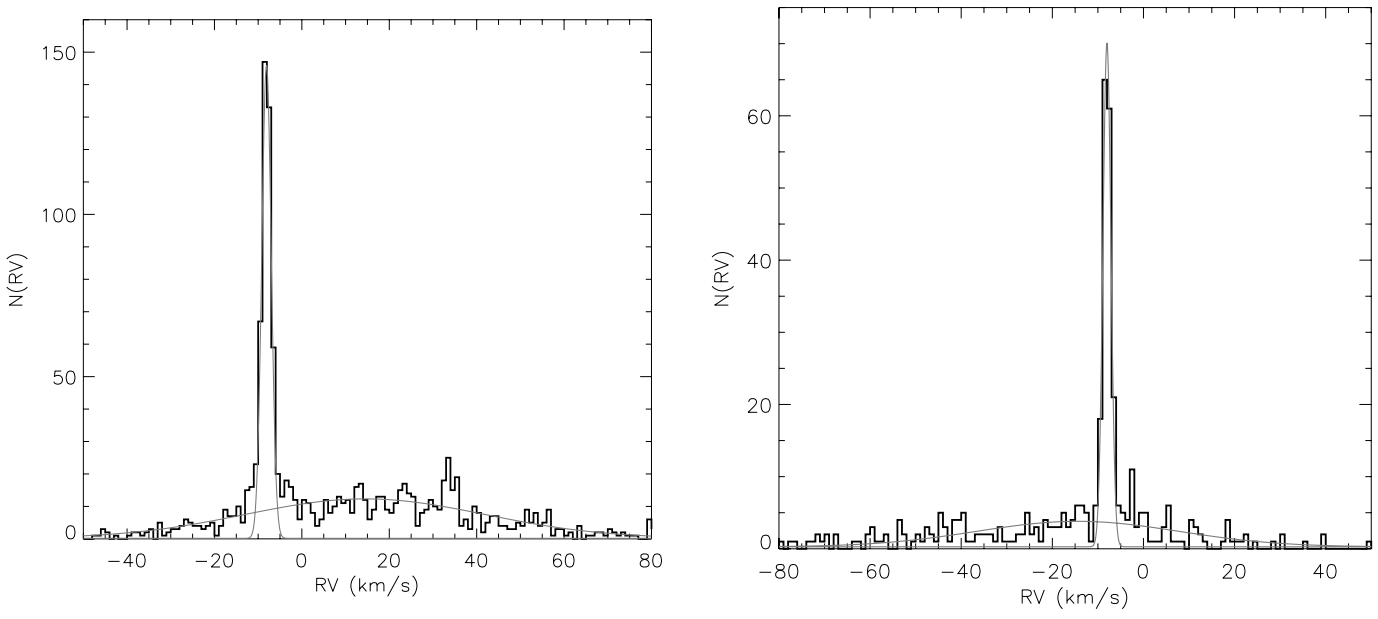

FIG. 3.—Distributions of radial velocities for stars in the fields of M35 (*left*) and M34 (*right*). Two Gaussian functions (*gray solid curves*) have been simultaneously fitted to the cluster and field components of each distribution.

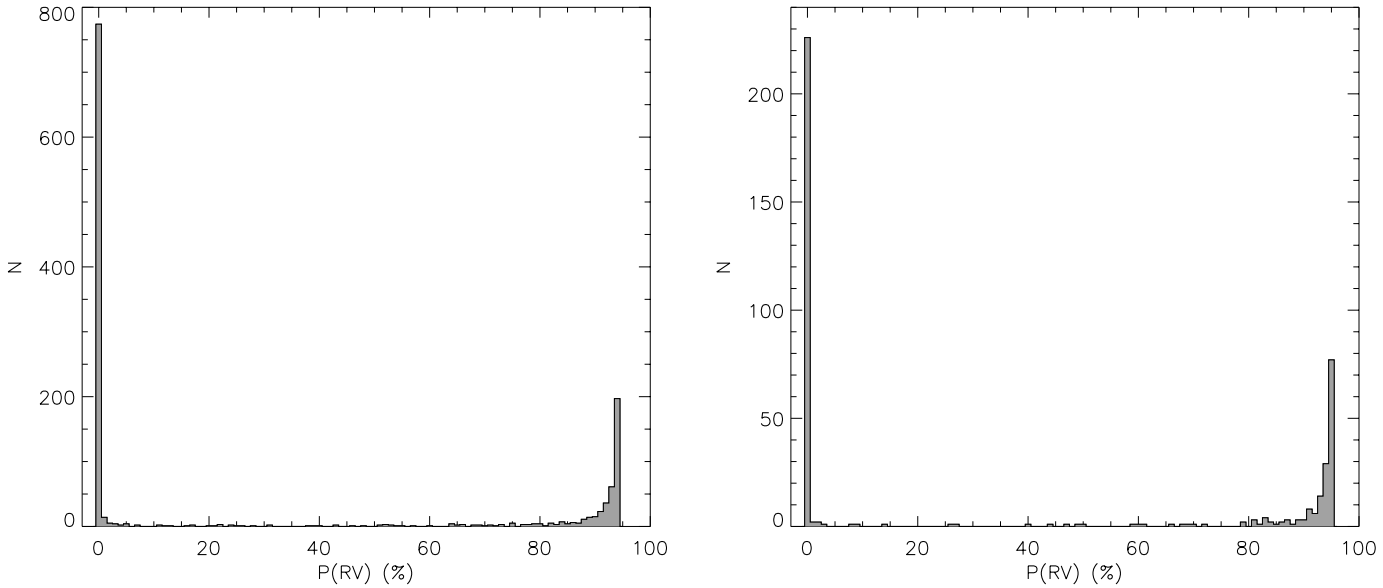

FIG. 4.—Distributions of radial velocity membership probabilities [$P(\mathrm{RV})$] for stars in the fields of M35 (*left*) and M34 (*right*). Cluster members and nonmembers are easily identified as two distinct peaks in the distributions. The space between the peaks is populated by stars with radial velocities corresponding to the wings of the cluster distributions.

where $C(\mathrm{RV})$ and $F(\mathrm{RV})$ represent the values of the Gaussian fit to the cluster and field distributions, respectively, for the center-of-mass radial velocity of a binary.

Figure 4 shows the distributions of radial velocity membership probabilities for stars in the fields of M35 and M34. In both clusters the separation between members and nonmembers is distinct. Less than 10% of the stars have probabilities placing them between the member and nonmember peaks, corresponding to radial velocities on the wings of the cluster distributions.

Of particular interest to our study of tidal synchronization are the six binaries with orbital periods in the range from 2.25 to 12.28 days. The stars in these six systems are close enough that their spins and orbits have evolved due to tidal interactions. Of the six, the orbital parameters for the five M35 binaries were first presented in Meibom & Mathieu (2005). The photometric light curves are presented here, and the derived rotation periods are listed in Table 1. The uncertainty ($\pm\delta P$) on the rotation periods were determined using the expression for the periodogram resolution (Kovacs 1981):

$$\delta P = P^2 \frac{3\sigma}{4T\sqrt{N}A}, \qquad (6)$$

where σ is the uncertainty in the photometric data, T is the total time spanned by the data, N is the number of independent data points, and A is the amplitude of the detected signal. When estimating rotation period uncertainties we made the conservative assumption that only data from separate nights are truly independent and set the value of N to the number of nights of data in the light curve. We describe here in detail the observational results for those six systems.

Binary 1455.—Fourteen radial velocity measurements have been obtained of this binary over ~600 orbital cycles. With an orbital period of only 2.25 days, this is the shortest period binary found in our survey of M35. The orbit is very near circular, with $e = 0.010 \pm 0.003$. Figure 5 shows the orbital solution overplotted on the radial velocity data phased to the 2.25 day period. The CMD location of binary 1455 is on the cluster main sequence slightly above the position on the 150 Myr isochrone corresponding to a mass of ~0.9 $M_\odot$. We use 0.9 $M_\odot$ as an estimate for the mass of the primary star, as there is no sign of the secondary star in the spectra/cross-correlation function of this binary. The radial velocity cluster membership probability (P_{RV}; eq. [5]) of binary 1455 is 94%.

The light curve and phased light curve shown in Figure 6 are based on 96 photometric measurements obtained over 15 nights in 2002 December. The maximum periodogram power corresponds to a period of 2.29 ± 0.02 days. We note that phasing the photometric measurements with the binary orbital period of 2.25 days rather than the independently determined value of 2.29 days produces only a subtle change of the light curve. When including the queue data, a total of 156 measurements were obtained from 2002 October to 2003 March. The same rotation period was found using all 156 measurements, but the phased light curve is noisier, presumably due to the varying quality of

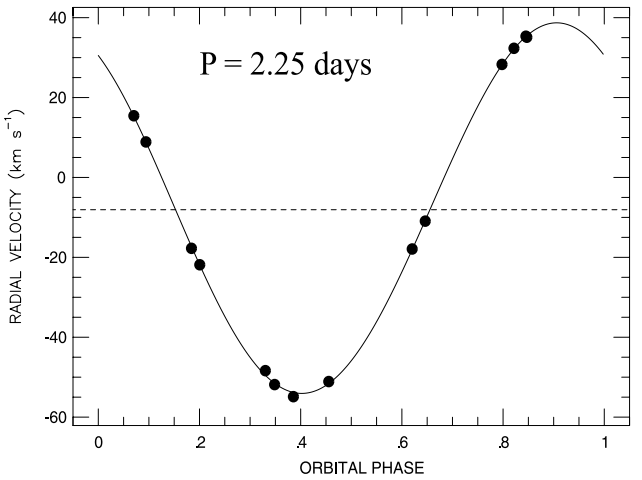

FIG. 5.—Radial velocity measurements of binary 1455 phased to an orbital period of 2.25 days. The best-fit orbital solution is overplotted. The orbit is very near circular, with an eccentricity of only 0.010 ± 0.003.

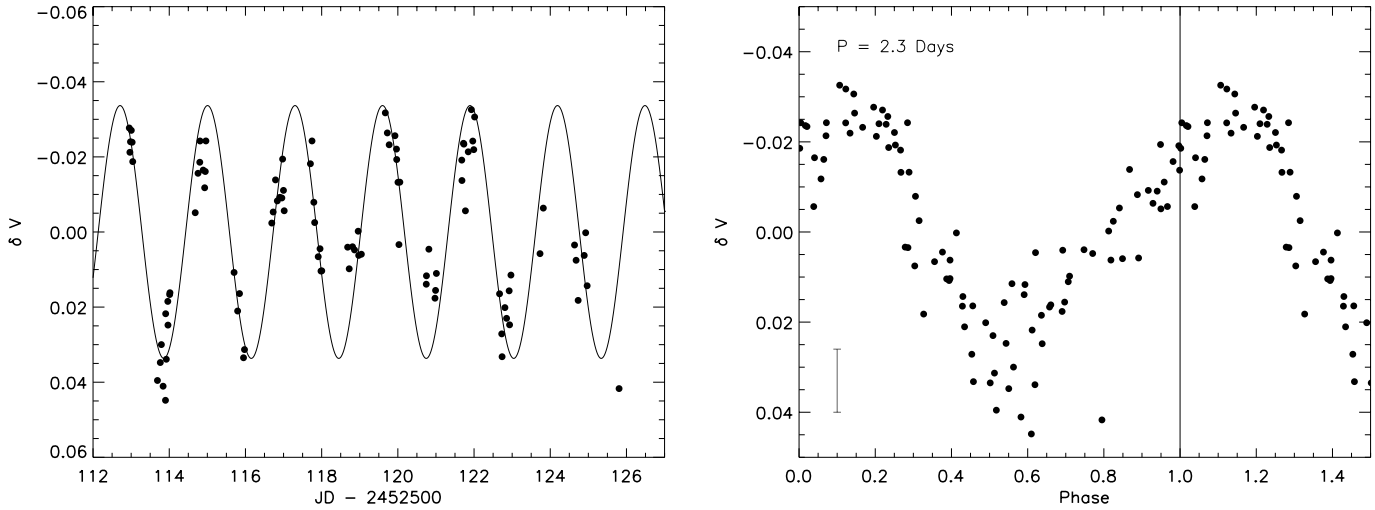

FIG. 6.—*Left*: Light curve for binary 1455 based on 96 photometric measurements from 15 nights in 2002 December. A sine function with a 2.29 day period overplotted. *Right*: Differential *V*-band photometry for binary 1455 phased to a period of 2.29 ± 0.02 days, corresponding to the maximum periodogram power. The vertical solid line indicates a phase value of 1.0, and the error bar in the lower left-hand corner represents plus and minus the typical photometric error at the *V* magnitude of binary 1455.

the queue data and possibly due to irregularities in the spot modulation over the longer timescale.

Binary 6211.—Figure 7 shows the orbital solution overplotted on 15 radial velocity measurements over ~160 orbital cycles. The data have been phased to a 4.39 day period. The orbit is indistinguishable from circular with an eccentricity of 0.063 ± 0.033. We estimate the mass of the primary star to be $\sim 0.7\ M_{\odot}$ using the fit of a 250 Myr Yale isochrone to the M34 cluster sequence. The radial velocity cluster membership probability of binary 6211 is 94%.

The light curve and phased light curve shown in Figure 8 are based on 55 photometric measurements over 15 nights. The data were kindly provided by S. A. Barnes (2005, private communication). The maximum power in the periodogram corresponds to a period of 8.03 ± 0.1 days. We note that phasing the photometric measurements with the binary orbital period of 4.39 days does not lead to well-phased data.

Binary 0422.—The radial velocity of this binary has been measured 41 times over ~330 orbital cycles. The high eccentricity of the orbit makes it difficult to observe during the short periastron passage. One observation has been obtained close to periastron passage, allowing a better determination of the orbital eccentricity. The cross-correlation function from this observation revealed a second spectral component with peak height about two-thirds that of the primary peak and a radial velocity of -8.8 km s^{-1}, consistent with the cluster radial velocity. We suggest therefore that this is a triple system consisting of a close binary and a distant tertiary star. The radial velocity curve for the binary, phased to a period of 8.17 days, is shown in Figure 9. The velocity of the presumed tertiary star is marked as a circle at phase 0.04. Overplotted is the best-fit orbital solution with an eccentricity of 0.649 ± 0.022. The center-of-mass velocity is -6.14 km s^{-1} ($\sim 2\sigma_{\rm cluster}$ away from the -8.1 km s^{-1} cluster velocity), corresponding to a radial velocity membership probability of 76%. This deviation from the cluster velocity may be partly due to the dynamical influence of the triple system. The system is located ~0.5 mag above the cluster main sequence, likely due to the combined light of the close binary and the tertiary star. Because the tertiary star is fainter than the primary in binary 0422, we assume that it is also redder and we estimate the mass of the primary star in binary 0422 by assuming that in the absence of the tertiary star the binary will be on the main sequence fainter and bluer than the triple system. We note, however, that these assumptions have no large effect on the estimated mass of the primary star.

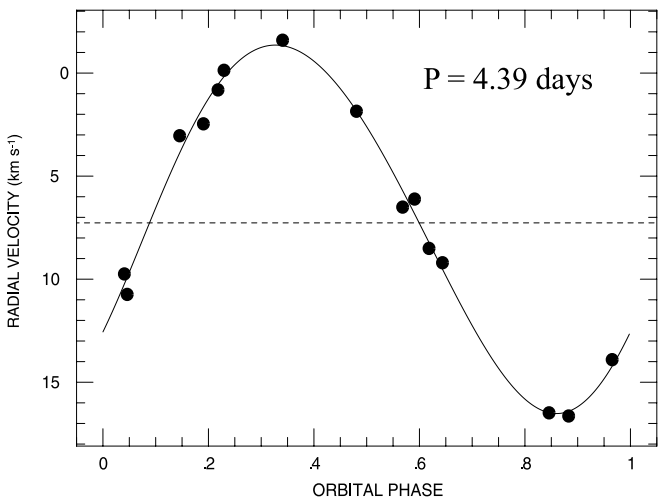

FIG. 7.—Radial velocity measurements of binary 6211 phased to an orbital period of 4.39 days. The best-fit orbital solution is overplotted. The orbit is circular, with an eccentricity of 0.063 ± 0.033.

Binary 0422 was imaged 126 times, 74 of which fell within 15 nights in 2002 December. The light curve and phased light curve shown in Figure 10 are based on those 74 photometric measurements. The rotation period corresponding to the maximum periodogram power is 3.71 ± 0.06 days. A slightly shorter rotation period of 3.56 days is found using all 126 photometric measurements, but the light curve is noisier. Again, the added noise is presumably due to the varying quality of the synoptic data and possibly due to irregularities in the spot modulation over the longer timescale.

Binary 0447.—The orbital parameters of this binary were determined from 32 radial velocity measurements over ~150 orbital cycles. The 10.28 day orbit is circular, with an eccentricity of 0.009 ± 0.019. Figure 11 shows the orbital solution overplotted on the phased radial velocity data. The color and *V* magnitude of binary 0447 places it on the cluster main sequence at the blue

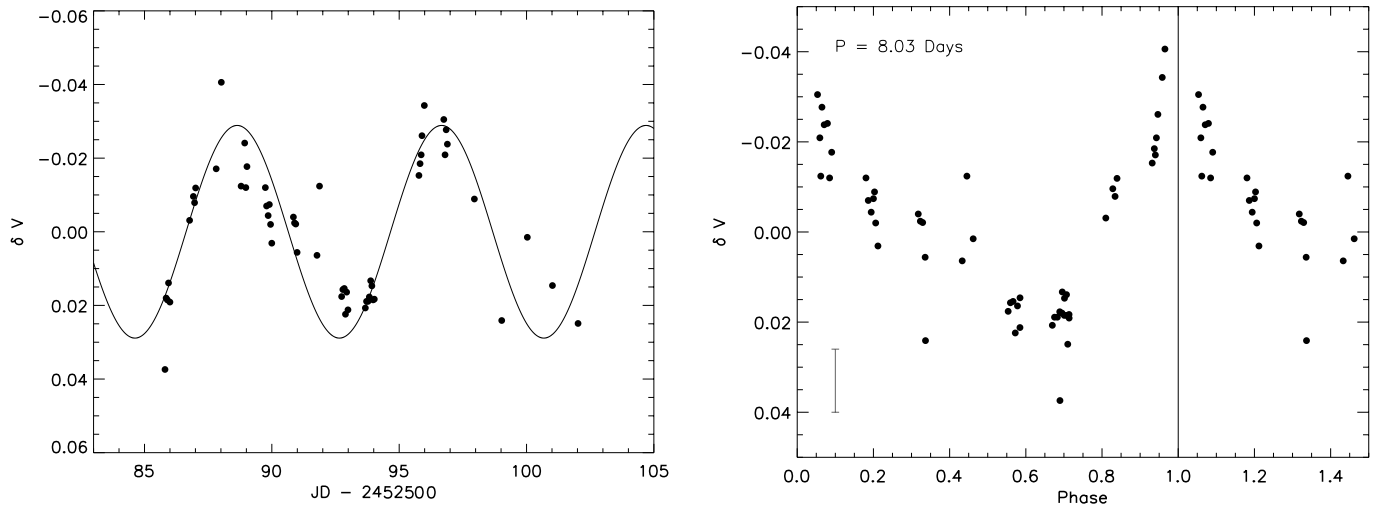

FIG. 8.—*Left*: Light curve for binary 6211 based on 55 photometric measurements kindly provided by S. A. Barnes (2005, private communication). A sine function with a period of 8.03 days is overplotted. *Right*: Differential *V*-band photometry for binary 6211 (S. A. Barnes 2005, private communication) phased to a period of 8.03 ± 0.1 days. The vertical solid line indicates a phase value of 1.0, and the error bar in the lower left-hand corner represents plus and minus the typical photometric error at the *V* magnitude of binary 6211 (S. A. Barnes 2005, private communication).

limit of our sample of M35 stars. This position corresponds to a mass of ~1.4 $M_\odot$ on the 150 Myr Yale isochrone. The radial velocity cluster membership probability is 94%. Furthermore, the measured lithium abundance for this star is consistent with cluster membership (Steinhauer & Deliyannis 2004).

The light curve and phased light curve shown in Figure 12 are based on 84 photometric measurements from the 15 nights in 2002 December. The rotation period corresponding to the maximum periodogram signal is 2.30 ± 0.02 days. A slightly shorter rotation period of 2.2 days is found when including the synoptic data.

Binary 6200.—Like binary 0447, this binary has a circular orbit ($e = 0.016 \pm 0.009$) with a period of ~10 days. Figure 13 shows the orbital solution overplotted on the radial velocity data phased to the 10.33 day period. The orbital parameters are determined from 22 radial velocities over ~120 orbital cycles. The location of binary 6200 on the M35 cluster sequence corresponds to a mass of ~1.1 $M_\odot$. The radial velocity cluster membership probability is 93%.

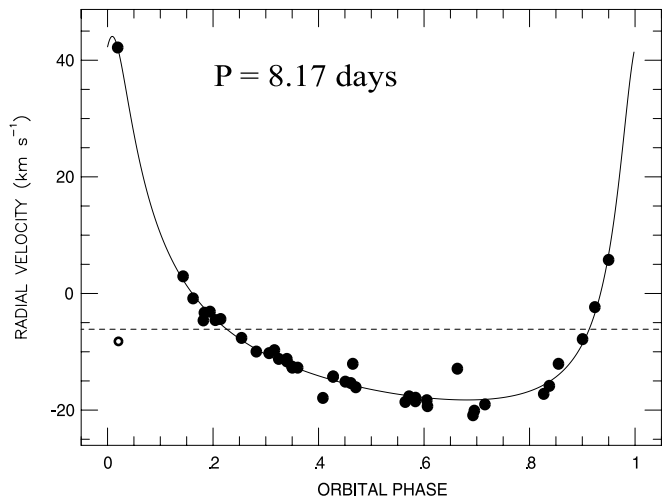

FIG. 9.—Radial velocity measurements of binary 0422 phased to an orbital period of 8.17 days. The best-fit orbital solution is overplotted. The orbit is highly eccentric ($e = 0.649 \pm 0.022$). One observation was obtained at periastron passage (maximum velocity separation), revealing a third spectral component. The velocity of the tertiary component is marked as an open circle at phase 0.04.

Figure 14 shows the light curve and phased light curve of binary 6200 based on 86 photometric measurements from 2002 December. A total of 138 measurements were made from 2002 October to 2003 March. The maximum periodogram power corresponds to a period of 10.13 ± 0.39 days. The same period was found using all 138 brightness measurements, but the periodic signal is noisier. We note the structure in the light curve between phase 0.6 and 0.8. This secondary signal is presumably due to a second group of photospheric spots.

Binary 3081.—The orbital solution for binary 3081 is based on 19 radial velocity measurements over ~70 cycles, and gives an orbital period of 12.28 days and an orbital eccentricity of 0.550 ± 0.003. Figure 15 shows the orbital solution overplotted on the phased radial velocity data. We estimate the mass of the primary star to be ~1.1 $M_\odot$. The radial velocity cluster membership probability is 93%.

Figure 16 shows the light curve and phased light curve based on 133 photometric measurements from 2002 December. The rotation period corresponding to the maximum periodogram power is 6.03 ± 0.12 days. The grouping of the data in the phased light curve is caused by the integer value of the rotation period and the data sampling frequency. The *V* magnitude of binary 3081 is 14.37, and its amplitude of variability is 0.02 mag, approximately 4 times the expected photometric error (see Fig. 2).

5. THE POTENTIAL PHOTOMETRIC EFFECTS OF BINARITY

Tidal synchronization is driven by dissipation within the star. Models of synchronization are thus sensitive to the stellar interior structure. To properly constrain such models, observations of tidal synchronization must be obtained for stars with known masses (structure). For single-lined spectroscopic binaries only the mass of the primary star can be determined. However, the brightness variations in a binary may be caused by effects other than spots on the surface of the primary star. We are not concerned with stellar eclipses, as they produce a characteristic and easily detectable photometric effect that with little difficulty can be distinguished from spot modulation. Still, other phenomena may cause photometric variability similar to that of spots on the primary star. We

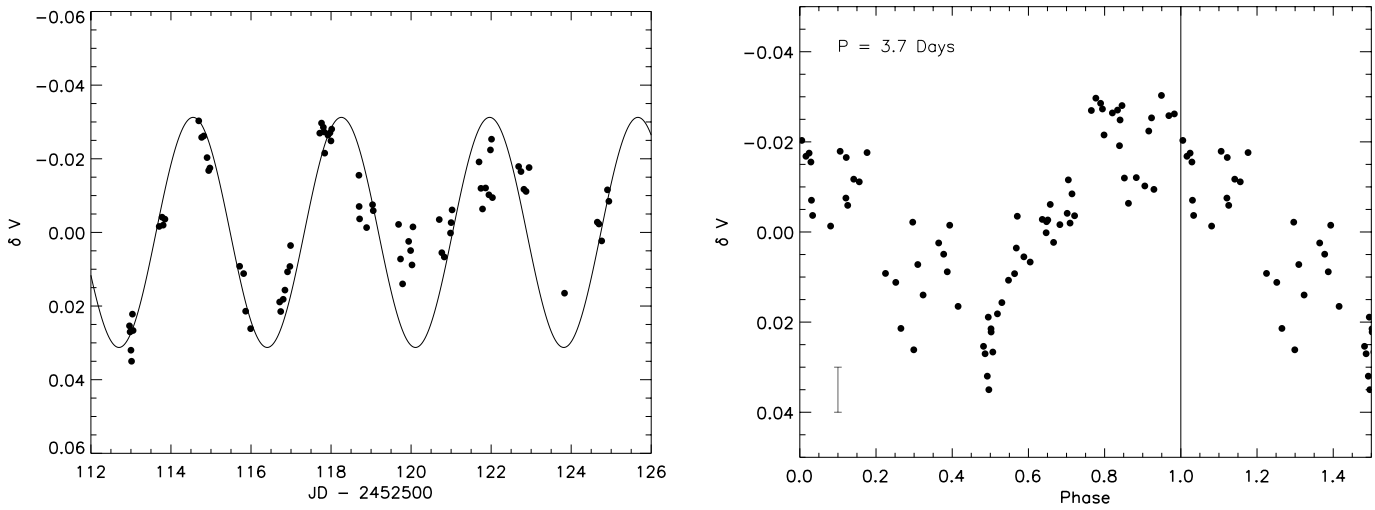

FIG. 10.—*Left*: Light curve for binary 0422 based on 74 photometric measurements from 2002 December. A sine function with a 3.71 day period is overplotted. *Right*: Differential *V*-band photometry for binary 0422 phased to a period of 3.71 ± 0.06 days. The vertical solid line indicates a phase value of 1.0, and the error bar in the lower left-hand corner represents plus and minus the typical photometric error at the *V* magnitude of binary 0422.

identify here two potential sources of photometric variability and estimate the influence of each of these effects on our ability to determine the rotation period of the primary stars from spot modulation.

5.1. *The Effect of Spots on the Secondary Star*

Let us first consider the effect of a spot on the surface of the secondary star. Because all of the binaries presented here are single-lined spectroscopic binaries, we assume that the *V*-band (∼5000 Å) flux of the secondary star is at least a factor of 5 less than that of the primary. We further assume that the spot on the secondary star produces an observed peak-to-peak brightness variation of the secondary of 0.15 mag in the *V* band, equivalent to the largest periodic signals observed in M35. The spot on the secondary, by itself, will then result in a 0.02 mag peak-to-peak variation in the brightness of the binary.

The observed peak-to-peak brightness variations of the binaries presented in this paper are in the range from ∼0.02 to 0.12 mag. Therefore, to assign the observed variability of these binaries to spots on the secondary will require the combination of a heavily spotted secondary star (flux reduction of up to 75%) and a quiet (spotless) primary star. Such a combination seems unlikely. The detected photometric variability is thus likely to result from spots on the primary star.

If, in a binary, both stellar spins have been synchronized or pseudosynchronized to the orbital motion, then photometric variability at the ∼0.02 mag level can be due to spots on both stars that appear in phase as seen by the observer. Arguably, stars in the majority of young solar-type binaries rotate out of phase and nonsynchronous with their eccentric orbital motion. The variability, if any, in the combined light of such binaries will derive from an out-of-phase superposition of the periodic signals caused by spots on both stars. Photometric time-series studies of solar-type main-sequence stars typically detect periodic variability at the level of ∼0.02–0.2 mag, and we know from the results presented here that such photometric variability is not confined to single stars. Therefore, we argue that the photometric variability detected in this and other studies comes from one star, either a single star or the primary star in a binary system.

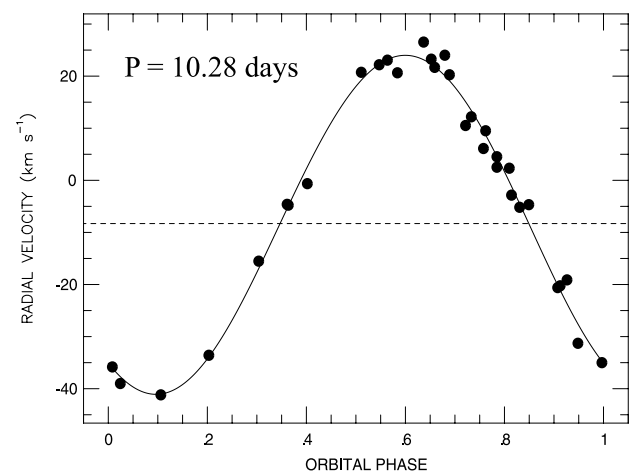

FIG. 11.—Radial velocity measurements of binary 0447 phased to an orbital period of 10.28 days. The best-fit orbital solution is overplotted. The orbit is circular ($e = 0.009 \pm 0.019$).

5.2. *The Effect of Tidal Deformation*

Another potential source of brightness variability in a binary star is the change in brightness due to tidally induced changes in the projected surface area of the stars. When a star becomes oblate due to the gravitational forces in the binary systems, its projected surface area, as seen by an observer, will change as it revolves. The change in area will depend on the binary mass ratio, the stellar separation, and the inclination of the orbit to the line of sight. For a circularized binary the resulting brightness variation will be sinusoidal with a period equal to half the orbital period. For a binary with an eccentric orbit, the brightness will increase at periastron passage and the light curve will deviate from a sinusoidal shape.

Zahn (1992) estimates the elevation, δR, of a tide on a star with mass M and radius R raised by a companion with mass m at a distance d, as $\delta R/R \simeq q(R/d)^3$, where $q = m/M$ is the binary mass ratio. If we assume that $M = 1.0\ M_\odot$ and $m = 0.7\ M_\odot$ and that the orbital period is 2.25 days (as in our shortest period binary), then $d = 0.04$ AU and $\delta R \simeq 0.08\ R_\odot$. To estimate an upper limit on the consequent photometric variation, we assume that the binary is seen "edge on" ($i = 90^\circ$), and that the radius of the stellar disk increases/decreases by δR when the line joining

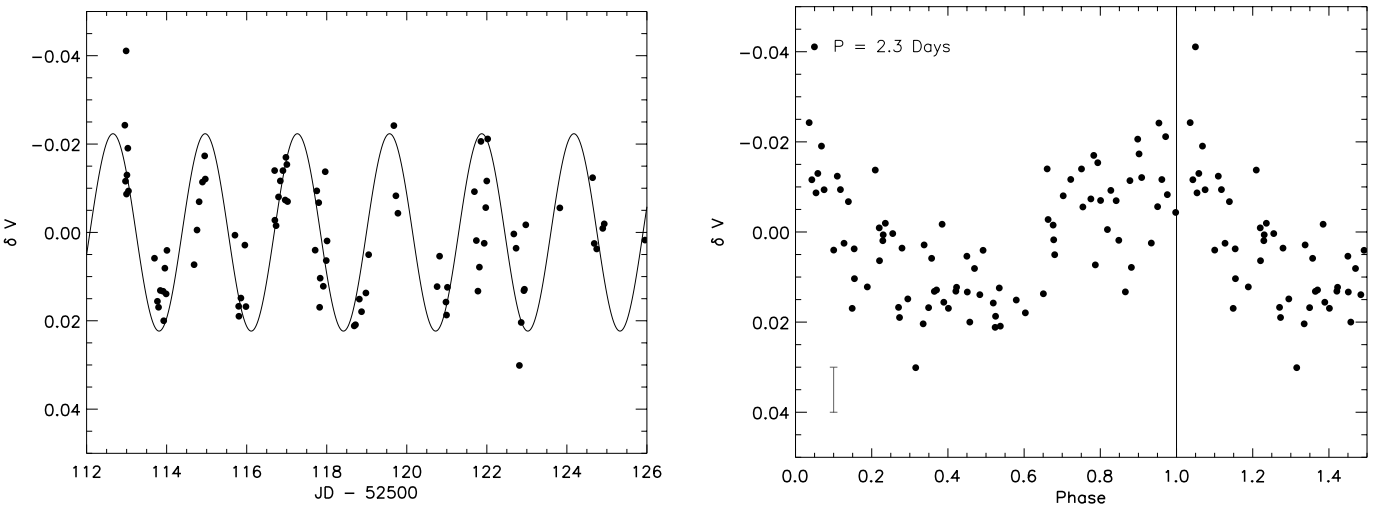

FIG. 12.—*Left*: Light curve for binary 0447 based on 84 photometric measurements from 2002 December. A sine function with a 2.30 day period is overplotted. *Right*: Differential *V*-band photometry for binary 0447 phased to a period of 2.30 ± 0.02 days, corresponding to the maximum periodogram power. The vertical solid line indicates a phase value of 1.0, and the error bar in the lower left-hand corner represents plus and minus the typical photometric error at the *V* magnitude of binary 0447.

the two stars is perpendicular/parallel to the line of sight. The resulting maximum difference in projected surface area of both stars corresponds to a brightness difference of ∼0.02 for the binary.

Note that this upper limit estimate for the variability introduced by tidal distortion is for a stellar separation corresponding to our shortest period binary. The effect will decrease rapidly with stellar separation and thus will be negligible for all binaries other than 1455. Binary 1455 has a 2.25 day circular orbit, and so the photometric variability due to tidal distortion in this system should have a period of 1.125 days and an amplitude of ≳0.02 mag. The light curve of 1455 actually varies with a period of 2.3 days and with an amplitude of 0.08 mag.

We conclude from this analysis that the periodic variability detected in the light curves of the unevolved single-lined M35 and M34 binaries are caused by spots on the solar-type primary stars, and are therefore reliable measures of their rotation periods. Thus, in what follows, we compare our observations of tidal synchronization to models using solar-type binary components.

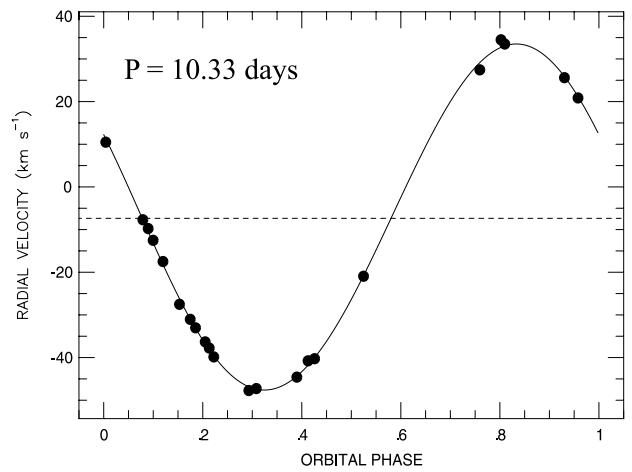

FIG. 13.—Radial velocity measurements of binary 6200 phased to an orbital period of 10.33 days. The best-fit orbital solution is overplotted. The orbit is circular ($e = 0.016 \pm 0.009$).

6. THE $\log(\Omega_\star/\Omega_{\rm ps})$-$\log(P)$ DIAGRAM

In this section we present our observational results in a way that facilitates comparison with predictions of tidal theory. In that spirit, we introduce in Figure 17 the $\log(\Omega_\star/\Omega_{\rm ps})$-$\log(P)$ diagram. From our observational results we can derive for each binary the average orbital angular velocity ($\omega = 2\pi/P_{\rm orb}$) and the rotational angular velocities of the primary star ($\Omega_\star = 2\pi/P_{\rm rot}^{\rm prim}$). With reference to § 2 and equations (3) and (4), we can calculate, for a given binary, the theoretical pseudosynchronization angular velocity ($\Omega_{\rm ps}$). As a diagnostic of the degree of tidal synchronization in a binary system we use the ratio of $\Omega_\star$ to $\Omega_{\rm ps}$,

$$\frac{\Omega_\star}{\Omega_{\rm ps}} = \frac{[1 + 3e^2 + (3/8)e^4](1 - e^2)^{3/2}}{1 + (15/2)e^2 + (45/8)e^4 + (5/16)e^6} \frac{P_{\rm orb}}{P_{\rm rot}^{\rm prim}}. \quad (7)$$

The base 10 logarithm of $\Omega_\star/\Omega_{\rm ps}$ [i.e., $\log(\Omega_\star/\Omega_{\rm ps})$] has a useful behavior for analysis. Synchronous and pseudosynchronous binaries will lie on the line represented by $\log(\Omega_\star/\Omega_{\rm ps}) = 0$. We refer to that line as the "synchronization line." Super-synchronous binaries ($\Omega_\star > \Omega_{\rm ps}$) will have $\log(\Omega_\star/\Omega_{\rm ps}) > 0$, while subsynchronous binaries ($\Omega_\star < \Omega_{\rm ps}$) have $\log(\Omega_\star/\Omega_{\rm ps}) < 0$. Figure 17 shows $\log(\Omega_\star/\Omega_{\rm ps})$ for all 13 binary stars as a function of their orbital periods and Table 1 lists the values of $\Omega_\star/\Omega_{\rm ps}$ and $\log(\Omega_\star/\Omega_{\rm ps})$. The uncertainties on both the orbital periods and on $\log(\Omega_\star/\Omega_{\rm ps})$ are small, and the error bars fit within the plotting symbols for all binaries with periods shortward of 100 days. We discuss here the degree of tidal synchronization in each of the six binaries with orbital periods less than 13 days.

Binary 1455.—The similarity of the orbital period (2.25 days) and the rotation period of the primary star (2.29 ± 0.02 days) suggests that the primary in binary 1455 is synchronized to the circular orbital motion. Binary 1455 is thus both tidally circularized and synchronized at the age of 150 Myr, and lies on the synchronization line in Figure 17 ($\Omega_\star/\Omega_{\rm ps} = 0.98$).

Binary 6211.—This 250 Myr M34 binary has a circular orbit with a period of 4.39 days, but the primary star is rotating subsynchronously at 8.03 ± 0.1 days, corresponding to 53% of the orbital angular velocity [$\Omega_\star/\Omega_{\rm ps} = 0.53$, $\log(\Omega_\star/\Omega_{\rm ps}) = -0.28$].

Binary 0422.—This 150 Myr M35 binary has not been circularized and has a highly eccentric orbit ($e = 0.65$) with a period of 8.17 days. The primary star in 0422 is not pseudosynchronized

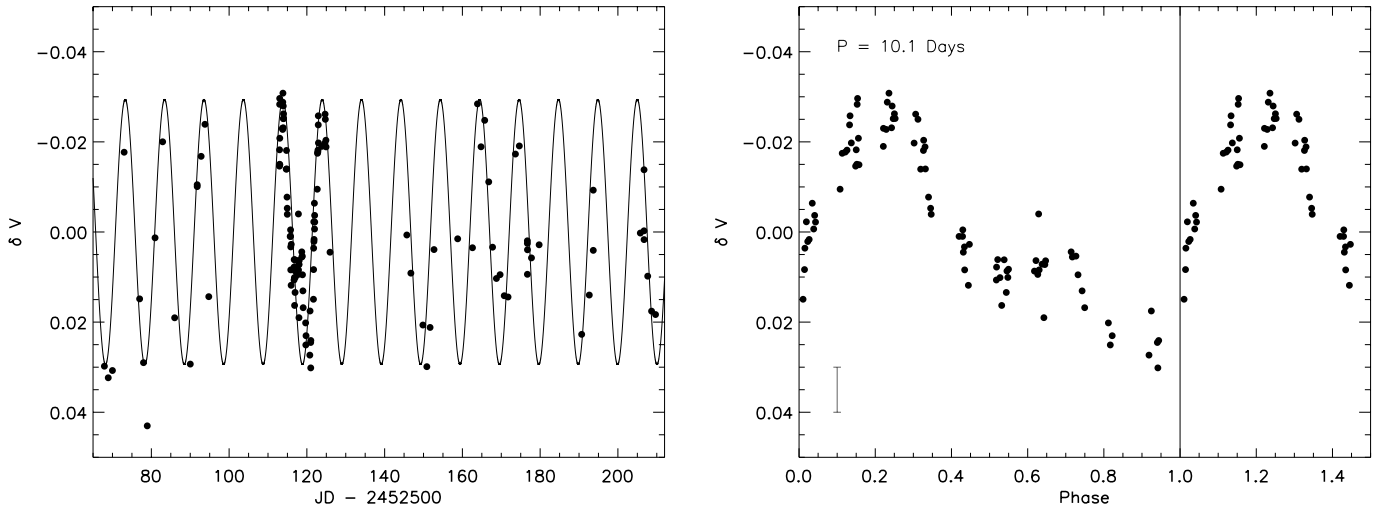

FIG. 14.—*Left*: Light curve for binary 6200 based on 138 photometric measurements from 2002 October to 2003 March. A sine function with a 10.13 day period overplotted. *Right*: Differential *V*-band photometry for binary 6200 phased to a period of 10.13 ± 0.39 days, corresponding to the maximum periodogram power. The vertical solid line indicates a phase value of 1.0, and the error bar in the lower left-hand corner represents plus and minus the typical photometric error at the *V* magnitude of binary 6200.

and rotates with a sub pseudosynchronous period of 3.71 ± 0.06 days, corresponding to 44% of Ω_{ps} [$\Omega_\star/\Omega_{ps} = 0.44$, $\log(\Omega_\star/\Omega_{ps}) = -0.35$]. Due to the relative brightness of the primary and tertiary star in this system, we cannot exclude the possibility that the detected photometric variability is due to spots on the tertiary (see discussion in § 5.1). In that case, spot activity on the primary star must be negligible, as the power spectrum resulting from the photometric data shows only one peak aside from the typical low-level signal due to the sampling of the data (the window function). We assume in the discussion below that the derived rotation period represents that of the brightest star in the system, the primary.

Binary 0447.—The 10.28 day orbit of this M35 binary is circular. The rotation period of the primary star is supersynchronous at 2.30 ± 0.02 days [$\Omega_\star/\Omega_{ps} = 4.46$, $\log(\Omega_\star/\Omega_{ps}) = 0.65$].

Binary 6200.—This M35 binary has a circular 10.33 day orbit and synchronized primary star. The primary star is rotating once every 10.13 ± 0.39 days corresponding to $\Omega_\star/\Omega_{ps} = 1.02$ or $\log(\Omega_\star/\Omega_{ps}) = 0.01$.

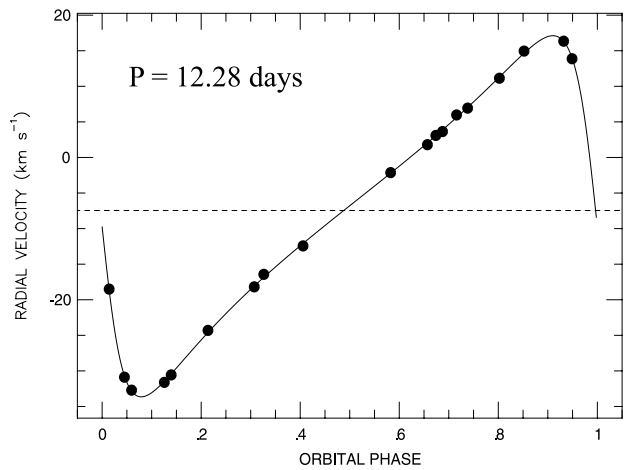

FIG. 15.—Radial velocity measurements of binary 3081 phased to an orbital period of 12.28 days. The best-fit orbital solution is overplotted. The eccentricity of the orbit is 0.550 ± 0.003.

Binary 3081.—The primary star of this M35 binary follows a highly eccentric ($e = 0.55$) orbit with a period of 12.3 days, while its rotation period of 6.03 ± 0.12 days correspond to subsynchronous rotation [$\Omega_\star/\Omega_{ps} = 0.61$, $\log(\Omega_\star/\Omega_{ps}) = -0.21$].

The rotation periods of the primary stars in the M35 binaries 422 and 3081 are approximately half their respective orbital periods. This result is interesting in light of the known effect of "period doubling," where two spots/spot groups $\sim 180^\circ$ apart on the stellar surface cause the observed period to be half the true period. While period doubling does occur (e.g., Stassun et al. 1999; Herbst et al. 2002), examinations of the power spectra and phased light curves do not support doubling of the rotation periods. We note also that binaries 422 and 3081 are highly eccentric, and doubling the rotation periods of the primary stars will not bring these systems into pseudosynchronization.

7. COMPARISON TO THEORETICAL EXPECTATIONS

Explicit predictions for tidal evolution based on the equilibrium or dynamical theories (§ 2) are published for only a few initial orbital and stellar parameters (see Zahn & Bouchet 1989; Witte & Savonije 2002). Ideally, model predictions would exist for a fine grid of such parameters, allowing for direct comparison with the different binaries observed in M35 and M34. In the absence of such a detailed theoretical framework, we must compare our observations of tidal evolution to predictions derived from more general findings of tidal theory. One such finding is the difference in the timescales for tidal synchronization and tidal circularization in a given binary system. Primarily due to the difference between stellar and orbital angular momenta, the timescale for tidal synchronization is approximately 2–3 orders of magnitude smaller than the timescale for tidal circularization for constant stellar structure. In lieu of specific theoretical predictions for the tidal evolution of our binaries, we use these relative timescales to formulate two simple expectations for tidal evolution in a coeval sample of *main-sequence* binaries: (1) the rotation of a star in a circularized binary should be synchronized to the orbital angular velocity; and (2) the rotation of a star in an eccentric binary should be pseudosynchronized ($\Omega_\star = \Omega_{ps}$) if the orbital period is similar to or shorter than the tidal circularization period.

While these simple expectations are likely valid for older main-sequence stars, the models of (Zahn & Bouchet 1989) caution that

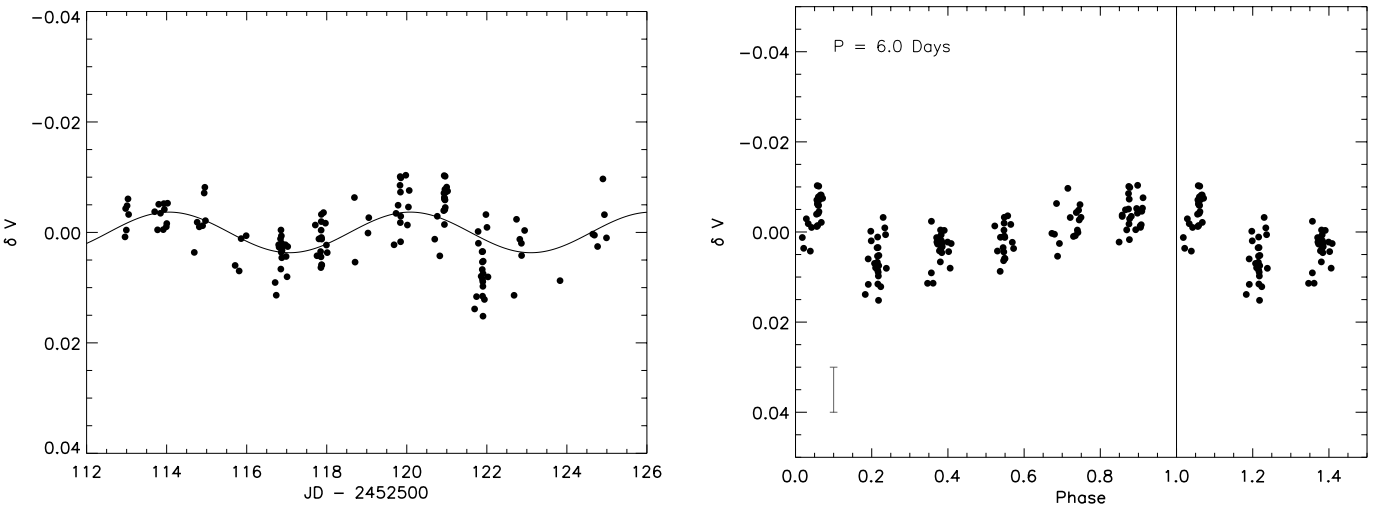

FIG. 16.—*Left*: Light curve for binary 3081 based on 133 photometric measurements from 2002 December. A sine function with a 6.03 day period is overplotted. *Right*: Differential *V*-band photometry for binary 3081 phased to a period of 6.03 ± 0.12 days, corresponding to the maximum periodogram power. The vertical solid line indicates a phase value of 1.0, and the error bar in the lower left-hand corner represents plus and minus the typical photometric error at the *V* magnitude of binary 3081.

primary stars in binaries as young as those studied here may be supersynchronously rotating to a small degree that depends on the initial stellar and binary parameters.

In the log $(\Omega_\star/\Omega_{\rm ps})$-log (P) diagram for M35 and M34, these expectations correspond to all of the shortest period binaries

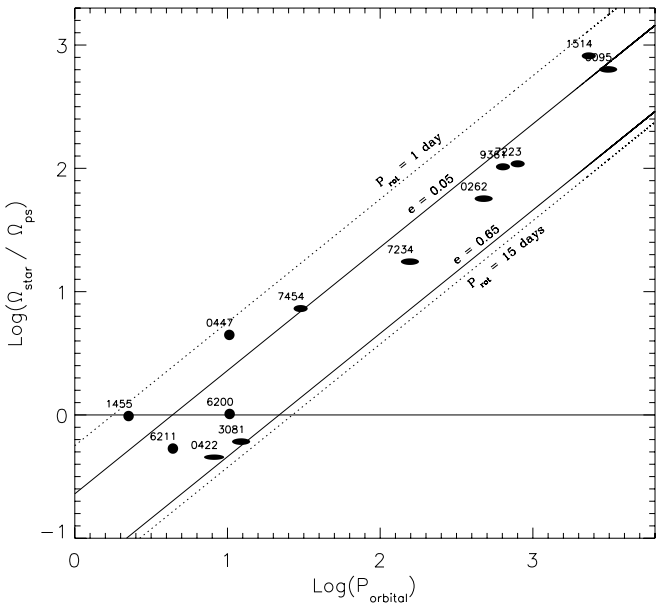

FIG. 17.—The log $(\Omega_\star/\Omega_{\rm ps})$-log (P) diagram for M35 and M34. Here log$(\Omega_\star/\Omega_{\rm ps})$ is plotted as a function of orbital period for all 13 binaries. The shape of the plotting symbols are indicative of the orbital eccentricity of each binary. A solid horizontal line (the synchronization line) mark log $(\Omega_\star/\Omega_{\rm ps}) = 0$, the location in the diagram for synchronized or pseudosynchronized binaries $(\Omega_\star = \Omega_{\rm ps})$; log $(\Omega_\star/\Omega_{\rm ps}) > 0$ for supersynchronous binaries and log $(\Omega_\star/\Omega_{\rm ps}) < 0$ for subsynchronous binaries. The interval framed by solid lines represents log $(\Omega_\star/\Omega_{\rm ps})$ corresponding to $P_{\rm rot}^{\rm prim} = 4.3$ days and $0.05 < e < 0.65$. The interval framed by dotted lines represents log $(\Omega_\star/\Omega_{\rm ps})$ corresponding to $e = 0.35$ and 1 day $< P_{\rm rot}^{\rm prim} < 15$ days. It is expected that binary primary stars, unaffected by tidal evolution, will be distributed in the area of the log $(\Omega_\star/\Omega_{\rm ps})$-log (P) diagram enclosed by the dotted lines. However, tidal theory predicts that primaries in binaries with periods similar to or shorter than the tidal circularization period $(10.2^{+1.0}_{-1.5}$ days) should be either (pseudo-) synchronized or rotate slightly supersynchronous and thus fall on or slightly above the synchronization line. The deviation from synchronization line of four of the six primaries with log $(P) \lesssim$ 1.2 thus offer interesting challenges to our understanding of tidal evolution in solar-type binaries.

$(P_{\rm orb} \lesssim 13$ days) being located either on the synchronization line or slightly above $(\Omega_\star/\Omega_{\rm ps} \lesssim 0.2)$. Inspection of Figure 11 immediately shows that this is not the case.

The two shortest period binaries, 1455 in M35 and 6211 in M34, both have circular orbits, as expected. Furthermore, the primary star of the shortest period binary, 1455, is indeed synchronized, in agreement with the first expectation. In marked contrast, the primary star of 6211 is rotating subsynchronously in a circular orbit, and thus runs counter to the most basic expectation of main-sequence tidal evolution. We note that the circular orbit of 6211 is not a surprise; in M34 the 4.4 day period is less than half that of the tidal circularization period of the younger M35, and three additional circular binaries have been found in M34 with periods between 4 and 5.5 days. Thus, it is the newly discovered subsynchronism that requires explanation.

The M35 binaries 0447 and 6200 provide another important comparison. Both have circular orbits at essentially the same 10.3 day period. However, the primary star of 6200 is rotating synchronously, as expected, while the primary of 0447 is rotating supersynchronously by more than a factor of 4. This high degree of supersynchronism is unexpected based both on the circular orbit of 0447 and on comparison with 6200, its near twin in period, eccentricity, and age. Perhaps of importance is the difference in the primary masses; 1.4 $M_\odot$ for 0447 and 1.1 $M_\odot$ for 6200. This difference in mass, and thus interior structure, of the primary stars can potentially translate into a difference in the mechanism and efficiency for tidal dissipation, in the internal angular momentum transport, and in the rate of external angular momentum loss (e.g., wind loss). Binaries 0447 and 6200 thus provide a remarkable test of the role of stellar mass and structure in tidal evolution.

The third diagnostic pair of binaries are the M35 eccentric binaries 0422 and 3081. Binary 0422 has a period of 8.17 days, shorter than the tidal circularization period of M35, yet retains an eccentricity of 0.65. 3081 has a period of 12.3 days, slightly longer than the M35 tidal circularization period, and has an eccentricity of 0.55. Both binaries represent the best cases in our sample to study evolution to pseudosynchronization. In fact, neither have achieved pseudosynchronization; both are rotating subsynchronously by factors of 2.2 and 1.7. As such, they both are counter to the second expectation of pseudosynchronism for periods near the tidal circularization period.

The primaries of three of these six binaries are observed to rotate subsynchronously. Stellar differential rotation and spots at high latitudes could lead to observed subsynchronous rotation not representative of the rotation at the stellar equator. Using the Sun as a reference, the difference in rotation period between the equator (25 days) and a latitude of 60° (32 days) of a solar-type star is 7 days. The angular rotation velocity determined from brightness variations due to a spot at 60° latitude will thus be about 25% less than if the spot were located at the equator. Assuming that this is the case for the primary stars in binaries 6211, 0422, and 3081, and thus increasing $\Omega_\star$ of the primary stars in these binaries by 25% leads to $\Omega_\star/\Omega_{\rm ps}$ ratio of 0.66, 0.75, and 0.57, respectively, for binaries 6211, 3081, and 0422. Such corrections are not sufficient to bring these binaries into synchronous or pseudosynchronous rotation. We conclude from these estimates that the subsynchronous rotation observed in the three binaries cannot be explained due to differential rotation and spots at high latitude unless differential rotation with latitude is more severe in younger stars as compared to the Sun.

To summarize, among six young (150–250 Myr), short-period (<13 days), solar-type binaries, only two have reached the equilibrium state of both a circularized orbit and synchronized rotation. Among the exceptions, we find binaries with circular orbits that are not synchronized (one being supersynchronous and one subsynchronous), and binaries with eccentric orbits that are not pseudosynchronized (both being subsynchronous). As a set, these six binaries present a challenging case study for tidal evolution theory. Here we begin that conversation with brief considerations of stellar evolution, stellar dynamics, tidal evolution theory, and initial conditions. None is capable of explaining all of the binaries.

Given the young ages of M34 and M35, these solar-mass stars have not been on the main sequence for long; hence the assumption of constant interior structure likely should be abandoned and the impact of PMS evolution considered. In fact, supersynchronous rotation ($\Omega_\star/\Omega_{\rm ps} \simeq 0.2$) at the age of M35 is predicted by Zahn & Bouchet (1989) for a circular 7.8 day period binary comprising two 1 $M_\odot$ stars. In their model the supersynchronous rotation on the early main sequence is a result of a weakened tidal torque as the convective envelope of the primary retreats during late PMS evolution. Consequently the primary star is not tidally locked as its radius decreases, and the star spins up as it evolves to the main sequence. Perhaps this is the explanation for the supersynchronous rotation of binary 0447. In this scenario its difference from binary 6200 would be attributed to a smaller convective envelope of the higher mass primary star in 0447, and thus relatively less tidal coupling than in 6200 since reaching the ZAMS. We note that the ratio of $\Omega_\star$ to ω for 0447 is almost 3 times the ratio predicted by Zahn & Bouchet at the age of M35, but their model calculation is for two solar-mass stars in any case. Indeed, arguably the synchronization of the 1.1 $M_\odot$ primary in the circularized 6200 with a 10.3 day period is a more significant contradiction with the Zahn & Bouchet model.

Our findings for the binaries 0422 and 3081 may also reflect on the dynamical evolution of the cluster. M35 is a rich cluster with a half-mass relaxation time of order 100 Myr (Mathieu 1983). It is likely that some binaries in the cluster core have gone through resonant gravitational encounters and stellar exchanges. Typically such encounters lead to hard, highly eccentric orbits for the binary products, and so perhaps the eccentric binaries 0422 and 3081 are such products. If so, the most massive stars—i.e., the primary stars—are the most likely to have been exchanged into the binary. As such, they would have experienced tidal torques for a time smaller than the age of the cluster, and indeed may retain their rotation periods from the time of the encounters. In this scenario, that both are subsynchronous is essentially the result of chance selection of those rotation periods from the single-star population.

Finally, we note that the null hypothesis that the rotation periods of the primary stars are not at all influenced by tidal effects cannot be definitively ruled out. We show in Figure 17 two intervals, one bounded by diagonal dotted lines and the other bounded by diagonal solid lines. The interval framed by solid lines represents $\log(\Omega_\star/\Omega_{\rm ps})$ corresponding to $P_{\rm rot}^{\rm prim} = 4.3$ days (the median observed rotation period for stars in M35; S. Meibom et al. 2006, in preparation) for $0.05 < e < 0.65$ (the observed range of nonzero orbital eccentricities in M35 Meibom & Mathieu 2005). The interval framed by dotted lines represents $\log(\Omega_\star/\Omega_{\rm ps})$ corresponding to $e = 0.35$ (the mean of the observed eccentricity distribution in M35) and 1 day $< P_{\rm rot}^{\rm prim} <$ 15 days (the range in rotation periods in M35). All of the M34 and M35 primary stars with measured rotation periods fall within these intervals, and thus are not distinguishable from the rotation periods of single stars. For the binaries with periods greater than 30 days, we presume that the rotation periods of the primaries in fact are set by the same mechanisms as in the single stars.

Might the same be said for the six binaries with periods of less than 30 days? The low rotation periods of the primary stars in both of the eccentric binaries 0422 and 3081 might derive simply from the same causes of such periods in single stars. In fact, the rate of tidal evolution in high-eccentricity binaries may be slower than for binaries with low eccentricities. In a highly eccentric orbit tidal interactions are essentially confined to a short time interval around periastron passage. If the duration of the tidal perturbation at periastron passage is shorter than the convective turnover time, the efficiency of tidal coupling may be significantly reduced (Goodman & Oh 1997; Goldman & Mazeh 1991; Zahn 1989). Duquennoy et al. (1992) and Meibom & Mathieu (2005) conjecture that eccentric binaries with periods at or below the tidal circularization period, such as 0422 and 3081, might be the result of high primordial eccentricities ($e \gtrsim 0.7$). Perhaps the consequently reduced rate of tidal evolution has allowed the rotational evolution of the primary stars to be little different from that of single stars.

We find it far less plausible that the rotational evolutions of the primaries of the four binaries with circular orbits have not been altered by tidal effects. Two of these binaries (1455, 6200) would have to fall on the synchronization line by chance, while the circular orbits of the other two (6211, 447) are strong evidence for substantial action by tidal forces since the formation of the system. In fact, evidence that tidal synchronization has affected the rotational evolution of the closest binaries can be found in the "color-period" diagram for M35. Figure 18 shows the M35 color-period diagram; the stellar rotation periods plotted against their colors (see also Barnes 2003). For clarity in this context, broad gray curves are plotted to represent well-defined observed sequences of M35 members (the actual M35 color-period diagram can be found in Meibom [2006] and will be published in S. Meibom et al. [2006, in preparation]). The locations of the 12 M35 binaries discussed in this paper are overplotted. The primary stars in binaries 447, 3081, and 6200 rotate abnormally slowly, with periods close to twice that of similar M35 stars, while wider binaries (*open circles*) fall on or close to the sequences representing the typical M35 star. In the cases of binaries 447 and 6200 (synchronized), this abnormally slow rotation provides further evidence that tidal synchronization has affected their rotational evolution.

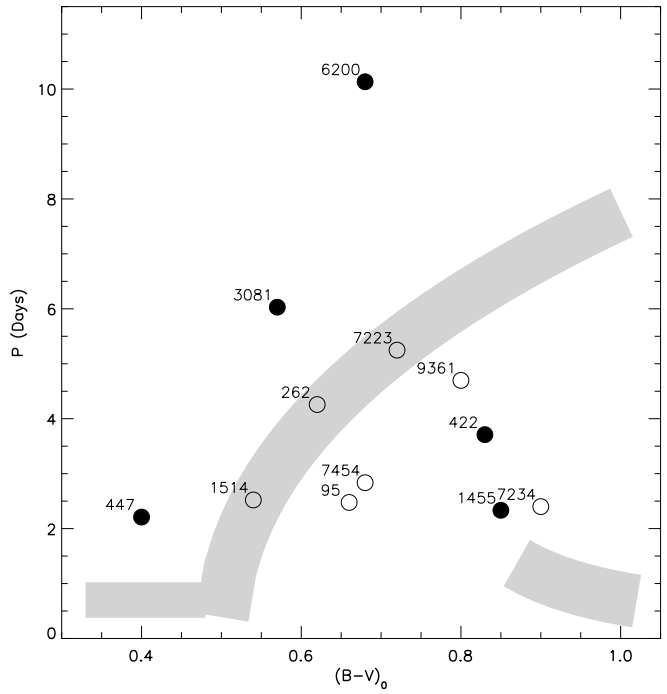

FIG. 18.—M35 color-period diagram-stellar rotation period plotted against the stellar color $(B - V)_0$. The broad gray curves represent well-defined observed sequences of M35 stars. The actual color-period diagram for M35 will be published in S. Meibom et al. (2006, in preparation). The locations of the 12 M35 binaries presented in this paper are overplotted as solid circles (five closest binaries) and open circles (seven wider binaries).

The observed rotational and orbital states of the six close M35 and M34 binaries pose interesting and different challenges to current tidal theory. To properly test tidal theory, models must be run with stellar and binary parameters tailored to fit the observed systems. Furthermore, ingredients such as internal stellar angular momentum transport and external wind loss should be included in such models, as both helioseismic observations of the Sun (e.g., Goode et al. 1991; Eff-Darwich et al. 2002) and observations of rotation of late-type stars in general (e.g., Barnes 2003; Soderblom et al. 1993) suggest that angular momentum is transported between the convective envelopes and the radiative cores in such stars.

8. SUMMARY AND CONCLUSIONS

Tidal forces in close detached binaries drive an exchange of angular momentum between the stars and their orbital motions. With time a close binary system will approach an equilibrium state in which the stellar spin axes are aligned perpendicular to the orbital plane, the stellar spins are synchronized to the orbital motion, and the stellar orbits are circular.

Tidal theory makes predictions about rates of tidal evolution in close solar-type binaries. However, current models cannot account for the extent of tidal circularization observed in the oldest populations of solar-type binaries, indicating that the theoretical rates of tidal evolution are too small. The same models predict that the process of tidal synchronization proceeds faster than tidal circularization by about 2–3 orders of magnitude. Observations of tidal synchronization therefore provide an important additional constraint on these models and the dissipation mechanisms they employ. Importantly, observing the rate of tidal synchronization also promises to shed light on physical processes of stars such as internal and external angular momentum transport.

We present rotation periods for the solar-type primary stars in 13 single-lined binaries with known orbital periods and eccentricities. All 13 binaries are radial velocity and photometric members of the young open clusters M35 (150 Myr) and M34 (250 Myr). The stellar rotation periods are derived from high-precision (0.5%) relative time-series photometry obtained from two weeks of classically scheduled observations combined with ~6 months of queue-scheduled monitoring.

We compare the rotational angular velocity of each primary star ($\Omega_\star$) to the angular velocity required for the star to be (pseudo-) synchronized ($\Omega_{\rm ps}$). We use the value of $\Omega_\star/\Omega_{\rm ps}$ as a measure of the degree of tidal synchronization and present that measure as a function of the binary orbital period (P) in a $\log(\Omega_\star/\Omega_{\rm ps})$-$\log(P)$ diagram.

Our previous studies of tidal circularization in these clusters have shown that the orbits of binaries with periods of ~10 days and less have been altered by tidal interactions. Considering theoretical predictions that the rate of tidal synchronization exceeds that of tidal circularization by of order a factor of 10^2–10^3 for constant stellar interior structure, in the context of constant stellar structure we would expect that (1) circularized binaries would also be synchronized; and (2) the shortest period eccentric binaries would be pseudosynchronized. In the case of the solar-type stars in these two young clusters, the primaries have only recently reached the ZAMS, and one set of tidal evolution models predict such stars to still be rotating supersynchronously as a consequence of their PMS contraction. Thus, general theoretical considerations and one set of specific models lead to the expectation that all binaries with periods shortward of ~10 days would fall on or slightly above the synchronization line [$\log(\Omega_\star/\Omega_{\rm ps}) = 0$] in the $\log(\Omega_\star/\Omega_{\rm ps})$-$\log(P)$ diagram.

However, four of the six binaries in M35 and M34 with orbital periods less than ~13 days offer interesting challenges to our understanding of tidal evolution in solar-type binaries, as follows.

The 10.28 day orbit of M35 binary 0447 has been circularized, but the 1.4 $M_\odot$ primary star rotates highly supersynchronously. As an important comparison, the M35 binary 6200 ($M_{\rm prim} \simeq 1.1\ M_\odot$ has been both circularized and synchronized at an orbital period of 10.33 days.

Both primary stars in the highly eccentric M35 binaries 0422 ($M_{\rm prim} \simeq 0.9\ M_\odot$, $P_{\rm orb} = 8.17$ days) and 3081 ($M_{\rm prim} \simeq 1.1\ M_\odot$, $P_{\rm orb} = 12.28$ days) are rotating slower than their pseudosynchronization speeds.

Orbiting in a 4.39 day circular orbit, the 0.7 $M_\odot$ primary star in the M34 binary 6211 is also rotating subsynchronously.

Only binaries 1455 and 6200 meet the expectations of tidal theory of synchronized primary stars in circular orbits. Nevertheless, the 10.33 day circularized orbit of binary 6200 contradicts models predictions of tidal circularization at 150 Myr (Meibom & Mathieu 2005).

At the present time, theoretical models make detailed predictions for only a few configurations of binary orbital and stellar parameters. Specific models must be run with carefully chosen initial orbital and stellar parameters to attempt to reproduce the observed tidal evolution at 150 and 250 Myr. Furthermore, future models of tidal evolution will face the challenges of incorporating the effects of internal and external angular momentum transport and perhaps the combined effects of the dynamical and equilibrium tides in late-type stars.

We propose explanations for the observed binary and stellar parameters within the framework of current theory of stellar and tidal evolution, stellar dynamics, and observed stellar and binary initial conditions. Specifically we suggest that the supersynchronous rotation of binary 0447 might be explained by PMS and

main-sequence tidal evolution (Zahn & Bouchet 1989) and the relatively high mass and shallow convection zone of the primary star. We also note that the subsynchronous rotation of the primary stars in binaries 0422 and 3081 might be due to either dynamical stellar interactions and/or reduced tidal dissipation in highly eccentric systems. We offer no explanation of the subsynchronous and circular binary 6211, but find it unlikely that the parameters of binary 6211 together with the three other circularized binaries are the result of chance initial conditions. Subsynchronous rotation has been predicted in close solar-type main-sequence binaries when loss of stellar angular momentum due to magnetic-wind braking is considered (Zahn 1994). However, only circular binaries were considered, and the predicted levels of subsynchronism were much smaller than observed here.

Populating the $\log(\Omega_\star/\Omega_{\rm ps})$-$\log(P)$ diagram with coeval homogeneous populations of binary stars sets the beginning of a new era in observational studies of tidal synchronization. With time, the $\log(\Omega_\star/\Omega_{\rm ps})$-$\log(P)$ diagram for binary populations spanning in age from the PMS to the late main-sequence phase will become an important observational tool tracing the evolution of tidal synchronization in a way similar to the e-$\log(P)$ diagram in studies of tidal circularization. While at this early time, the limited number of binaries that can be placed in the diagram does not allow us to determine a "tidal synchronization period" marking the transition between synchronous and asynchronous systems, the degree of tidal synchronization in individual binaries provide interesting challenges to tidal theory. The success of theoretical models can be measured by their ability to predict the observed orbital and rotational evolution of these binary stars.

We are grateful to the University of Wisconsin, Madison, for the time granted on the WIYN 0.9 and 3.5 m telescopes. We would like to express our appreciation for exceptional and friendly support of site managers and support staff at both telescopes. We are thankful to all observers in the WIYN 0.9 m consortium who provided us with high-quality data through the synoptic observing program. We thank Sydney Barnes for making the photometric measurements of binary 6211 available to us, Imants Platais for providing 2MASS IDs, and our colleagues at the Third Granada workshop on Stellar Structure Tidal Evolution and Oscillations in Binary Stars for fruitful discussions. We thank the referee for a careful review of the paper resulting in several insightful recommendations that strengthened the paper. This work has been supported by NSF grant AST 97-31302 and by a Ph.D. fellowship from the Danish Research Agency (Forskningstyrelsen) to S. M.

REFERENCES

Abt, H. A., & Boonyarak, C. 2004, ApJ, 616, 562
Abt, H. A., Levato, H., & Grosso, M. 2002, ApJ, 573, 359
Andersen, J. 1991, Astron. Astrophys. Rev., 3, 91
Barnes, S. A. 2003, ApJ, 586, 464
Claret, A. 1995, A&AS, 109, 441
Claret, A., & Cunha, N. C. S. 1997, A&A, 318, 187
Claret, A., & Gimenez, A. 1995, A&AS, 114, 549
Claret, A., Gimenez, A., & Cunha, N. C. S. 1995, A&A, 299, 724
Cudworth, K. M. 1971, AJ, 76, 475
Duquennoy, A., Mayor, M., & Mermilliod, J. C. 1992, in Binaries as Tracers of Stellar Formation, ed. A. Duquennoy & M. Mayor (Cambridge: Cambridge Univ. Press), 52
Eff-Darwich, A., Korzennik, S. G., & Jiménez-Reyes, S. J. 2002, ApJ, 573, 857
Giuricin, G., Mardirossian, F., & Mezzetti, M. 1984a, A&A, 131, 152
———. 1984b, A&A, 135, 393
———. 1984c, A&A, 141, 227
Goldman, I., & Mazeh, T. 1991, ApJ, 376, 260
Goode, P. R., Dziembowski, W. A., Korzennik, S. G., & Rhodes, E. J. 1991, ApJ, 367, 649
Goodman, J., & Dickson, E. S. 1998, ApJ, 507, 938
Goodman, J., & Oh, S. P. 1997, ApJ, 486, 403
Herbst, W., Bailer-Jones, C. A. L., Mundt, R., Meisenheimer, K., & Wackermann, R. 2002, A&A, 396, 513
Hole, K. T., Mathieu, R. D., Latham, D. W., & Meibom, S. 2006, AJ, submitted
Hut, P. 1981, A&A, 99, 126
Kalirai, J. S., Fahlman, G. G., Richer, H. B., & Ventura, P. 2003, AJ, 126, 1402
Kovacs, G. 1981, Ap&SS, 78, 175
Latham, D. W., Stefanik, R. P., Torres, G., Davis, R. J., Mazeh, T., Carney, B. W., Laird, J. B., & Morse, J. A. 2002, AJ, 124, 1144
Levato, H. 1974, A&A, 35, 259
Mathieu, R. D. 1983, Ph.D. thesis, Univ. California, Berkeley
———. 2000, in ASP Conf. Ser. 198, Stellar Clusters and Associations: Convection, Rotation, and Dynamos, ed. R. Pallavicini, G. Micela, & S. Sciortino (San Francisco: ASP), 517
Mathieu, R. D., Duquennoy, A., Latham, D. W., Mayor, M., Mermilliod, T., & Mazeh, J. C. 1992, in Binaries as Tracers of Stellar Formation, ed. A. Duquennoy & M. Mayor (Cambridge: Cambridge Univ. Press), 278
Mathieu, R. D., Meibom, S., & Dolan, C. J. 2004, ApJ, 602, L121
McNamara, B., & Sekiguchi, K. 1986, AJ, 91, 557
Meibom, S. 2006, Ph.D. thesis, Univ. Wisconsin, Madison
Meibom, S., Barnes, S. A., Dolan, C., & Mathieu, R. D. 2001, in ASP Conf. Ser. 243, From Darkness to Light: Origin and Evolution of Young Stellar Clusters, ed. T. Montmerle & P. André (San Francisco: ASP), 711
Meibom, S., & Mathieu, R. D. 2005, ApJ, 620, 970
Melo, C. H. F., Covino, E., Alcalá, J. M., & Torres, G. 2001, A&A, 378, 898
Ogilvie, G. I., & Lin, D. N. C. 2004, ApJ, 610, 477
Savonije, G. J., & Witte, M. G. 2002, A&A, 386, 211
Scargle, J. D. 1982, ApJ, 263, 835
Soderblom, D. R., Stauffer, J. R., MacGregor, K. B., & Jones, B. F. 1993, ApJ, 409, 624
Stassun, K. G., Mathieu, R. D., Mazeh, T., & Vrba, F. J. 1999, AJ, 117, 2941
Stassun, K. G., van den Berg, M., Mathieu, R. D., & Verbunt, F. 2002, A&A, 382, 899
Steinhauer, A., & Deliyannis, C. P. 2004, ApJ, 614, L65
Tassoul, J.-L. 1988, ApJ, 324, L71
———. 1987, ApJ, 322, 856
Terquem, C., Papaloizou, J. C. B., Nelson, R. P., & Lin, D. N. C. 1998, ApJ, 502, 788
Vasilevskis, S., Klemola, A., & Preston, G. 1958, AJ, 63, 387
von Hippel, T., Steinhauer, A., Sarajedini, A., & Deliyannis, C. P. 2002, AJ, 124, 1555
Witte, M. G., & Savonije, G. J. 2002, A&A, 386, 222
Yi, S. K., Kim, Y., & Demarque, P. 2003, ApJS, 144, 259
Zahn, J.-P. 1975, A&A, 41, 329
———. 1977, A&A, 57, 383
———. 1989, A&A, 220, 112
———. 1992, in Binaries as Tracers of Stellar Formation, ed. A. Duquennoy & M. Mayor (Cambridge: Cambridge Univ. Press), 278
———. 1994, A&A, 288, 829
Zahn, J.-P., & Bouchet, L. 1989, A&A, 223, 112